

2004

Investigation of the molecular basis for silicon biofunctionality

Wang, Jingpeng

<http://knowledgecommons.lakeheadu.ca/handle/2453/2798>

Downloaded from Lakehead University, Knowledge Commons

Lakehead University

An Investigation of the Molecular Basis for Silicon Biofunctionality

By

Jingpeng Wang

A Thesis

Submitted to the Faculty of Graduate Studies

In Partial Fulfilment of the Requirements for the

Degree of Master of Science

Department of Chemistry

Thunder Bay, Ontario



Library and
Archives Canada

Bibliothèque et
Archives Canada

Published Heritage
Branch

Direction du
Patrimoine de l'édition

395 Wellington Street
Ottawa ON K1A 0N4
Canada

395, rue Wellington
Ottawa ON K1A 0N4
Canada

Your file *Votre référence*
ISBN: 0-494-00497-5
Our file *Notre référence*
ISBN: 0-494-00497-5

NOTICE:

The author has granted a non-exclusive license allowing Library and Archives Canada to reproduce, publish, archive, preserve, conserve, communicate to the public by telecommunication or on the Internet, loan, distribute and sell theses worldwide, for commercial or non-commercial purposes, in microform, paper, electronic and/or any other formats.

The author retains copyright ownership and moral rights in this thesis. Neither the thesis nor substantial extracts from it may be printed or otherwise reproduced without the author's permission.

AVIS:

L'auteur a accordé une licence non exclusive permettant à la Bibliothèque et Archives Canada de reproduire, publier, archiver, sauvegarder, conserver, transmettre au public par télécommunication ou par l'Internet, prêter, distribuer et vendre des thèses partout dans le monde, à des fins commerciales ou autres, sur support microforme, papier, électronique et/ou autres formats.

L'auteur conserve la propriété du droit d'auteur et des droits moraux qui protègent cette thèse. Ni la thèse ni des extraits substantiels de celle-ci ne doivent être imprimés ou autrement reproduits sans son autorisation.

In compliance with the Canadian Privacy Act some supporting forms may have been removed from this thesis.

Conformément à la loi canadienne sur la protection de la vie privée, quelques formulaires secondaires ont été enlevés de cette thèse.

While these forms may be included in the document page count, their removal does not represent any loss of content from the thesis.

Bien que ces formulaires aient inclus dans la pagination, il n'y aura aucun contenu manquant.


Canada

Abstract

Despite advances in our understanding of the beneficial role of silicon in the biosphere, surprisingly little is known of the molecular mechanism by which silicon is absorbed, transported, accumulated and deposited by organisms. We used silicon-29 NMR spectroscopy to investigate the interaction of the rare amino acid 2,3-*trans*-3,4-*cis*-3,4-dihydroxy-L-proline (DHP) with aqueous silicon. Spectral data revealed the structure of three organosilicate complexes that DHP spontaneously forms with aqueous silicon at $\text{pH} \cong 7.9$, making DHP the first ever known Si-binding amino acid. Such a discovery has potential significance in accounting for silicon's biological role in hydroxyproline-rich structural glycoproteins found in both mammals and plants.

The cell wall morphology of wheat, *Triticum aestivum* L., grown in either -Si or +Si media was examined by optical and scanning electron microscopy. The preliminary results indicate that Si-deficiency causes swelling of the parenchyma cell walls, supporting the hypothesis that silicon may enhance cell wall integrity by cross-linking pectic polysaccharide molecules via complexation at the apiofuranose binding sites. Silicon-29 and ^{13}C NMR spectroscopy were used to test this theory at the molecular level.

Blood and urine were collected periodically from a human subject following ingestion of ^{29}Si -enriched silicic acid and analyzed by ICP-OES and NMR spectroscopy. In addition to studying the kinetics of Si uptake and excretion, we obtained the first

reliable speciation of Si-containing molecules in human biofluids, and demonstrated that mono- and disilicic acid are the predominant species.

Acknowledgments

I would like to express my sincere gratitude to Dr. Stephen D. Kinrade for his guidance during the course of this research. I also wish to thank Dr. C. Taylor (Massey University, New Zealand) for providing the DHP and ATDN molecules, Dr. D. Chapman for recording the data in the wheat cell wall study (and Figure 3.5.1), and Dr. E. Epstein and W. Rains (University of California) for growing the two sets of wheat plants. Meanwhile, I would like to appreciate the help from Dr. C. Knight (University of Illinois at Urbana-Champaign) for assistance with NMR techniques, Drs. J. Powell and R. Jugdaohsingh (King's College, UK) for providing the ICP-OES data and Dr. H. Perreault (University of Manitoba) for MS data. In addition, I would like to thank the members of the Lakehead University Instrumentation Laboratory for NMR training and ICP data, as well as all the past and present members of the Kinrade research group with whom I have had the pleasure of working.

Contents

Abstract.....	ii
Acknowledgments	iii
Contents	iv
Symbols and Abbreviation	vi
Abbreviations	vi
Symbols	vi
Chapter 1-Introduction	1
1.1 Silicon in Biology	1
1.2 Molecular Basis of Silicon Biofunctionality	10
i) Polyol Interactions with Aqueous Silicon	10
ii) Amino Acid Interactions with Aqueous Silicon	13
1.3 Rhamnogalacturonan II (RG-II) and Silicon's Influence on Plant Cell Walls.....	17
1.4 Silicon Uptake and Excretion in Humans	21
1.5 Silicon-29 NMR	22
Chapter 2-Experimental	24
2.1 General Sample Preparation	24
2.2 NMR Measurement	27
2.3 Speciation of Small Organosilicate Complexes	27
2.4 Isolation and Purification of Red Wine RG-II	31

2.5	Effect of Silicon on Cell Wall Morphology of Wheat (<i>Triticum aestivum</i>)	<u>33</u>
2.6	Analysis of Silicon Uptake and Excretion in Humans	<u>36</u>
Chapter 3-Results and Discussions		<u>39</u>
3.1	NMR Examination of the 4-Aminobutanol-Trypsin-Silicate System	<u>39</u>
3.2	Aqueous Silicon Interactions with 2,3- <i>trans</i> -3,4- <i>cis</i> -3,4-Dihydroxy-L-proline (DHP)	<u>41</u>
3.3	NMR Examination of D-apiose in Alkaline Silicate Solution.....	<u>54</u>
3.4	Isolation and Purification of Red Wine RG-II	<u>60</u>
3.5	Effect of Silicon on Cell Wall Morphology of Wheat (<i>Triticum aestivum</i>)	<u>63</u>
3.6	Analysis of Silicon Uptake and Excretion in Humans	<u>70</u>
Conclusions		<u>77</u>
Future Work		<u>79</u>
References		<u>80</u>
Appendix I		<u>99</u>
Appendix II		<u>100</u>

Symbols and Abbreviation

Abbreviations

ATDN	Ac-Tyr-DHP-NHMe
DDW	deionized distilled water (type I)
DHP	2,3- <i>trans</i> -3,4- <i>cis</i> -3,4-dihydroxy-L-proline
FEP	fluorinated Ethylene-Propylene
LDPE	low density polyethylene
ICP-AES	inductively coupled plasma-atomic emission spectrometry
ICP-OES	inductively coupled plasma-optical emission spectroscopy
NMR	nuclear magnetic resonance
RG-II	rhamnogalacturonan II
S.E.C.	size exclusion chromatography
SEM	scanning electron microscopy
TFE	tetrafluoroethylene

Symbols

δ	NMR chemical shift (ppm)
J	nuclear spin-spin coupling constant
K	equilibrium constant
T_1	spin-lattice relaxation time

Chapter 1 – Introduction

1.1 Silicon in Biology

Silicon is the second most abundant element in the Earth's crust after oxygen, usually occurring in the form of silica and silicate minerals and almost invariably with tetrahedral coordination to oxygen. Elemental silicon, although rare in nature, is sometimes found in fulgurites, which are fused tubules of sandy soil created by lightning strikes. Minerals containing SiO_6 octahedra (*e.g.*, stishovite) are associated with meteor impact events [1]. Although silicon is thus readily accessible in the biosphere [2], the true extent of its biological impact has only recently been recognized [3].

Silicon is known to be an essential element in the *classical* sense for only a small number of primitive organisms such as diatoms, radiolarians, horsetails and some sponges. Silicon is needed for these organisms to complete their respective life cycle [2]. However, many higher plant species (*e.g.*, vascular plants including grasses and cereals) require silicon to protect against a host of abiotic and biotic stresses (wilting, lodging, metal toxicity, salinity, temperature extremes, fungal diseases, insect damage) and to enhance the efficiency of photosynthesis [4]. For these plants, Si-deficiency

causes demonstrable abnormalities in growth, development, reproduction and overall viability. Epstein [4] argues that silicon should at the very least be recognized as “quasi-essential” in such cases. In animals, Si-deficiency has been linked to bone and connective tissue abnormalities [5], heart disease [6], cancers [7] and neurodegenerative disorders [8]. Some workers have suggested that silicon’s role is not biological, and is instead related to its ability to limit the bioavailability of toxic metals such as aluminum, copper and iron [3, 9-11].

The solubility of silica in aqueous solution is markedly pH dependent above pH 8.0 [12], but nearly constant across the *ca.* pH 5-8 range typical of groundwater and soil solutions — ranging from 5 ppm (8×10^{-5} mol L⁻¹) to 11 ppm for quartz and 100-130 ppm for amorphous silica in neutral water at 298 K. At these concentrations, silica exists primarily as monosilicic acid Si(OH)₄ (weakly acidic, $pK_{a1} = 9.8$) and, to a lesser extent, disilicic acid (OH)₃SiOSi(OH)₃ [13, 14]. However, as the Si concentration approaches the solubility of amorphous silica, a wide variety of rapidly interchanging, low molecular weight oligomers appear [15, 16]. The mechanism of silicate condensation has been studied intensively [17].

Solid silicates are not only formed by geological processes. A wide range of

organisms including protists, higher plants and animals [18] are known to produce amorphous hydrated SiO_2 , the second most abundant biogenic mineral after carbonate minerals [19]. Significant strides are being made towards unraveling the processes that govern the deposition of silica within organisms. The most studied species in the field of *biosilicification* (the process by which organisms capture and mineralize silica [20]) are diatoms, a phylum of unicellular algae that lives in marine and freshwater habitats [21]. They utilize silicon to create silicified cell walls (*frustules*), enhance photosynthesis and induce metabolic processes leading to the synthesis of certain proteins and DNA [22]. Each diatom species is characterized by a specific biosilica cell wall that contains regularly arranged slits or pores in the size range between 10 and 1000 nm [23]. Biosilica morphogenesis takes place inside the diatom cell within a specialized membrane-bound compartment termed the silica deposition vesicle or *SDV*. It has been postulated that the SDV contains a matrix of organic macromolecules that not only regulate silica formation but also act as templates to mediate biosilica nanopatterning [24].

Insight into the nature of this organic matrix has been gained through the characterization of certain biosilica-associated compounds extracted from different

diatom species. These macromolecules are long-chain polyamines and polycationic polypeptides termed *silaffins* [24-27], both of which have been shown to promote formation of silica nanospheres from silicic acid *in vitro* under neutral or even slightly acidic conditions [25, 28] similar to those reported for the diatom SDV [29].

Silaffin-1A, a low molecular weight silaffin isolated from *Cylindrotheca fusiformis*, consists mainly of post-translationally modified lysine and serine residues. Each serine residue is phosphorylated, and this high level of phosphorylation is essential for biological activity [30]. The lysines exist in three different derivative forms: ϵ -N-dimethyllysine; ϵ -N-trimethyl- δ -hydroxylysine; and lysine residues covalently linked to long-chain polyamines [31(b)]. These long-chain polyamines have linear chains of up to twenty N-methylated propylamine units that are attached to putrescine or some putrescine derivative [26]. Polyamines are known to affect silica formation in several ways [28, 31, 32]. They catalyze siloxane-bond formation and possibly act as templates or structure-directing agents in the SDV. Recently, a highly polyanionic phosphoprotein termed “native silaffin-2” (or natSil-2) was isolated from diatom biosilica [33]. Silaffin-2 lacks intrinsic silica formation activity, but is able to regulate the silica-forming activity of long-chain polyamines and silaffin-1A.

Long-chain polyamines have been found in all diatom species investigated. Silaffins also occur [25, 26], although they are not quite as ubiquitous as the polyamines [31]. Kröger *et al.* have proposed that these two groups of molecules self-assemble electrostatically to form the organic matrix used by diatoms to generate their porous biosilica patterns [33].

Silica-precipitating proteins also occur in sponges. The siliceous marine sponge *Tethya aurantia* deposits silica in needlelike spicules that support the organism and provide defense against predation. About 75% of the dry weight of *Tethya aurantia* is comprised of silica spicules (1-2 mm long, 30 μm in diameter), containing an axial central filament of protein (1-2 mm long, 2 μm in diameter) that is fully occluded within the silica [34]. These filaments can be isolated, purified and resolved into three very similar silicon-free subunits named silicatein α , β and γ . Each has been shown to be capable of catalyzing and structurally-directing the *in vitro* polymerization of silica and silsesquioxane $(\text{RSiO}_{3/2})_n$ polymeric networks from the corresponding alkoxide substrates $(\text{RSi}(\text{OEt})_3, \text{R} = \text{OEt}, \text{Me}, \text{Ph})$ at ambient temperature and neutral pH [35].

Analysis of the DNA sequence for silicatein α , which comprises about 70% of the mass of the filaments, revealed that this subunit is structurally related to members of

the cathepsin L and papain family of proteases [34]. Zhou *et al.* [35] suggested that the catalytic role of silicatein α is therefore similar to that of the homologous proteases, which activate the hydrolysis of peptide and ester bonds under neutral conditions. They proposed a detailed reaction mechanism in which the serine residue with hydroxymethyl side chain at position 26 and the histidine residue with imidazole side chain at position 165 are catalytically involved in the hydrolysis [35]. The macroscopic silicatein filaments are also thought to serve as scaffolds that organize the deposition and growth of the resulting silica and silsesquioxane products [35]. (For the sponge *Suberites domuncula*, Krasko *et al.* [36] reported that silicate influences the genes expression of the enzyme silicatein and collagen via the mediator myotrophin.) However, it has been questioned whether silicatein's ability to hydrolyze silicon alkoxides *in vitro* has any appreciable biological significance [37, 38].

Investigations into the nature of the biosilica matrix have also been performed on higher plants. Silicon is mostly absorbed by plants in the form of uncharged silicic acid $\text{Si}(\text{OH})_4$, the bulk of which is deposited irreversibly as amorphous ("opaline") silica phytoliths in cell walls throughout the plant. Although deemed a non-essential nutrient for the majority of plants, silicon uptake provides many benefits such as improvements to

pest and pathogen resistance [39], drought and heavy-metal tolerance [40-43], structural stability and photosynthetic capacity [44], as well as to the overall quality and yield of crops [45]. Moreover, excess silicon availability does not cause severe injury to plants [46]. Since the benefits of silicon absorption vary from species to species and are usually only apparent under conditions of biotic and abiotic stress, a comprehensive view of silicon plant biology and its role in plant health has not yet been formulated. Knowledge of silicon metabolism at the molecular level in higher plants even lags behind that in diatoms and sponges [37, 39].

Silicon absorption in higher plants is either thought to be a passive event that coincides with the uptake of water [47] or an active form of nutrient foraging [48, 49, 50]. Based on measurements of silicon content and transpiration rates, Ma *et al.* [46, 51, 52] assigned over 500 plant species into one of three categories: high silicon accumulators (active uptake or sequestration); intermediate silicon accumulators (passive uptake); or non silicon accumulators (rejective uptake). The relationship between silicon translocation and transpiration is complex [39], and no inference was made concerning the mechanism of uptake (*e.g.*, via channel, pump or carrier).

Similarly, the mechanism of silicon deposition in plants has yet to be

characterized. As in the case of diatoms and sponges, however, there is evidence to suggest that silica deposition occurs via H-bonding interactions with an organic matrix composed of proteinaceous macromolecules which contain hydroxylated amino acids and saccharides [17, 53]. Kauss *et al.* [54] recently reported a novel proline-rich protein expressed by cucumber seedlings in response to pathogen attack that catalyzes silica deposition at the site of attempted fungal penetration, presumably owing to the high density of positively-charged amino groups. The authors speculate on the general applicability of the mechanism in other green plants.

Only within the past few decades has it been recognized that silicon actively participates in the normal life processes of higher animals [55]. Connective tissues such as aorta, trachea, tendon, bone, cartilage and skin are unusually rich in silicon, as shown by studies in several species [56], thus inferring that silicon is an integral component of the glycosaminoglycans and collagens that contribute to the formation of connective tissues. Moreover, silicon-deficiency has been shown to result in the abnormal development of articular cartilage, connective tissues [57], skull [58] and long bone [59]. Carlisle *et al.* have suggested a mitochondrial role for silicon in the proline synthetic pathway [60], and that silicon regulates the activity of enzyme prolyl hydroxylase [61].

They have also noted that the Si level of osteogenic cells is generally high, especially in the osteoblast which is the cell's metabolically active state, providing additional support for silicon's metabolic role in connective tissue formation [62].

These intriguing findings have stimulated much research on silicon bioavailability in mammals including calves [63], dogs [64] and humans [65, 66]. Silicon supplementation of postmenopausal women with osteoporosis reportedly not only inhibited bone resorption, it increased both the trabecular bone volume [67] and bone mineral density [68]. These results are supported by studies with ovariectomized rats, the standard animal model for postmenopausal osteoporosis, in which oral silicon completely abrogated the loss of bone mass [69, 70]. Powell *et al.* [71] recently demonstrated a strong correlation between dietary silicon intake and increased cortical bone mineral density in both men and premenopausal women. Surprisingly, this correlation vanishes completely in the case of postmenopausal women. These same researchers showed that physiological concentrations of orthosilicic acid stimulates collagen type I synthesis in human osteoblast-like cells and enhances osteoblastic differentiation [72]. TanBeeWan *et al.* [73] subsequently determined that the closely related silicone degradation product, dimethylsilanediol, enhanced both the survival and

proliferation rate of human osteoblast-like Saos-2 cells.

1.2 Molecular Basis of Silicon Biofunctionality

i) Polyol Interactions with Aqueous Silicon

Despite advances in our understanding of the beneficial role of silicon in the biosphere, surprisingly little is known of the mechanism by which silicon is absorbed, transported, accumulated and deposited by organisms. While some workers speculated that inorganic silicon might be extracted and conveyed as a complex with organic compounds [74, 44], others were skeptical [3b] since there was no direct evidence of either Si-C or Si-O-C functionality occurring in nature. Only synthetic examples of organosilicon and organosilicate complexes were known to exist [75-78].

In aqueous solution, the only known instances of silicon directly interacting with organic molecules were those in which silicon is chelated by catechol [79], 2-hydroxypyridine N-oxide [80], tropolone [81], or their respective analogues under alkaline conditions, yielding organosilicate complexes containing a single hexaaxosilicon centre. In 1999, Kinrade and coworkers [82] identified a series of stable organosilicate complexes that form in aqueous alkaline silicate solutions upon addition of certain

aliphatic polyols (*e.g.*, mannitol, xylitol and threitol). The silicon centres in these organosilicate complexes are also not tetrahedral, existing instead with either penta- or hexa- coordination as indicated by the corresponding ^{29}Si NMR resonances at *ca.* -100 ppm and -140 ppm, respectively. Such hypercoordinated silicon-polyolate complexes only form when the binding ligand contains four or more adjacent hydroxy groups, with the centre pair in *threo* configuration. They are especially stable if the ligand also contains a carboxylic acid end group [83], so much so that they exist even in neutral solution at biologically relevant Si concentrations [84]. The 6-coordinated Si complexes tend to be favoured under highly alkaline conditions [82, 83]. Subsequent molecular orbital modeling studies [38, 85] indicated that the likely bonding sites on the acyclic polyols are the *threo* hydroxy pair, as was recently verified crystallographically by Benner *et al.* [86]. The resulting organosilicate molecules contain two or three 5-membered chelate rings, and the dimensional configuration of the non-coordinating hydroxy groups greatly enhance the overall stability (in the solid state, at least) by forming strong hydrogen bonds with ligating alkoxo functions [86].

Certain furanoidic molecules are also capable of binding silicon hypervalently [87, 88]. Silicon complexation occurs with 1,4-anhydroerythritol,

cis-1,2-dihydroxycyclopentane, ribose and with various ribonucleosides (*e.g.*, adenosine, cytidine, guanosine) and ribonucleotides (including ATP and NAD⁺), all of which possess *vicinal cis*-diol functionality [87]. Silicon-29 NMR spectra of solutions containing pentaoxosilicon complexes are generally characterized by three strong signals between *ca.* -97 and -102 ppm. Detailed analysis has revealed that these resonances correspond to three different diastereomers of the monomeric bis(diolato)-hydroxo complex, [(L=)₂SiOH]⁻ (where L represents the *cis*-diol ligand), in which the ligands are oriented in *syn,syn*, *anti,anti* or *syn,anti* configuration [88, 90(a)].

Having established that aqueous silicon is readily complexed by a wide variety of sugars and sugar derivatives, the Kinrade group and their collaborators proceeded to examine whether organosilicates might play a role in biological systems. First, they conducted an *in vivo* ²⁹Si NMR investigation of synchronized colonies of the freshwater diatom *Navicula pelliculosa* [89]. A weak ²⁹Si resonance was reproducibly observed at *ca.* -131.5 ppm about 6 h after the diatoms were fed ²⁹Si isotope, and assigned to a transient hexacoordinated organosilicate complex. This observation represented the first-ever direct evidence of a hypercoordinated organosilicate complex formed during the life cycle of an organism. Next, ²⁹Si NMR was employed to examine the chemical

speciation of silicon in the root exudate of wheat (*Triticum aestivum* L.) [50].

Significantly, there was no evidence of organosilicates; only monosilicic acid and disilicic acid were detected.

Boric acid has long been known to react with mono- and polyhydroxy hydrocarbons in aqueous solution to form stable mono- and polyolato-boron complexes not unlike those formed with aqueous silicon [90]. To date, several naturally occurring boroesters have been identified, including three microorganism-derived antibiotics [91], an extracellular signaling molecule in bacteria [92], and the plant cell wall oligosaccharide, rhamnogalacturonan-II or RG-II [93], which will be discussed later. In the present study, therefore, we looked to organoborate chemistry for clues to the molecular basis of silicon biofunctionality.

ii) Amino Acid Interactions with Aqueous Silicon

As discussed above, mechanisms proposed to account for the activity of silica-precipitating proteins in diatoms and sponges are based on direct interaction of their constituent amines and peptides with the silanol groups of silicic acid (or alkoxysilane). Although the electrostatic, hydrogen-bonding and hydrophobic influence

of the individual amino acids and oligopeptides on silica formation have been investigated [94], no stable complex containing an amino acid bound to silicon has ever been reported [38, 85]. Indeed, Kinrade *et al.* [95] could find no evidence of aqueous silicon binding to any of the 20 most common amino acids in alkaline solution.

A ternary borate-alcohol-trypsin complex was recently reported forming spontaneously in aqueous solution (Figure 1.2.1), a finding with important implications for the design of selective serine protease inhibitors [96, 97]. The boron centre in the resulting complex is esterified by the hydroxymethyl group on serine-195 of trypsin and the oxygen atom of 4-aminobutanol [96]. The formation mechanism for this stable complex, likely involving the imidazole nitrogen on histidine-57 of trypsin, is remarkably similar to that proposed for the silicatein-mediated silicification process — the active sites of silicatein α also being residues of serine and histidine (Figure 1.2.2) [35].

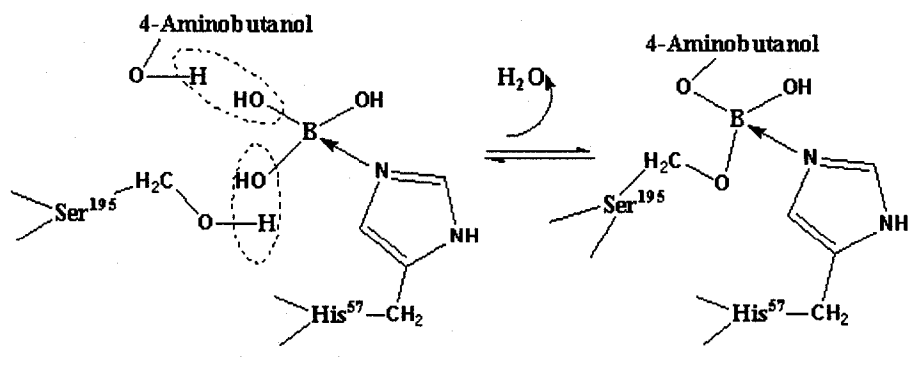


Figure 1.2.1 Speculated formation mechanism of trypsin-borate-4-aminobutanol ternary complex (after [96]).

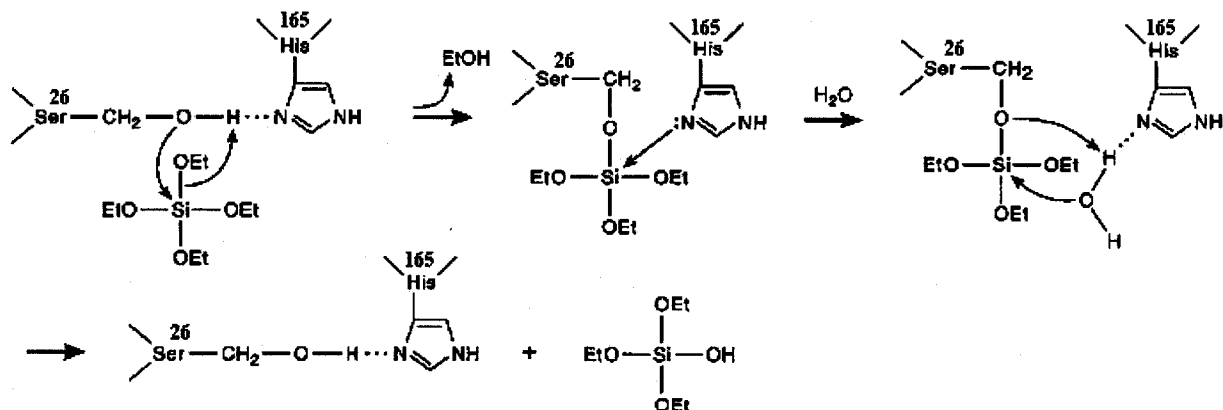


Figure 1.2.2 The proposed mechanism for silicatein-mediated catalysis of the alkoxy silane polycondensation (after [35]). The transitory protein-substrate intermediate is stabilized as a pentavalent silicon species through a donor bond from the imidazole nitrogen atom.

In the present study, we investigated a corresponding silicate-aminobutanol-trypsin system for evidence of any interaction that could support the mechanisms proposed to account for the activity of silica-precipitating proteins.

3,4-Dihydroxyproline (DHP) is the rarest of all amino (imino) acids. It contains three stereogenic centres, C2, C3, and C4, and consequently has eight possible stereoisomers (Figure 1.2.3). Three members of the L-series have been detected in nature [98]. The first to be isolated, 2,3-*cis*-3,4-*trans*-3,4-dihydroxy-L-proline (**1**), was obtained over 30 years ago from hydrolysates of a cell wall protein of the diatom *Navicula pelicullosa* [99]. The 2,3-*trans*-3,4-*trans*-3,4-dihydroxy-L-proline (**2**) was

isolated in 1980 from acid hydrolysates of the toxic mushroom *Amanita virosa* and identified in the virotoxin cyclic heptapeptides [100]. In 1994, the 2,3-*trans*-3,4-*cis*-3,4-dihydroxy-L-proline (**3**) was identified as the sixth residue in the repeating decapeptide sequence of *Mytilus edulis* foot protein 1 (Mefp1), a tremendously strong adhesive protein produced by the common blue marine mussel [101] and thought to have significant commercial applications [102]. This latter isomer is a strong candidate for Si-complexation, being the nitrogen analogue of furanoidic *cis*-diol molecules such as ribose. Waite and Tanzer [103] reported the isolation of Mefp1 as early as 1981, and later on proposed amino acid sequences for the commonly repeated fragments [104]. In 1994, Taylor and Waite [101] unveiled a revised sequence for the repeating unit (Figure 1.2.4), in which the sixth residue was properly identified as *trans*-2,3-*cis*-3,4-dihydroxyproline instead of the originally proposed *trans*-3-hydroxyproline.

In the present study, we characterized the interaction of aqueous silicon with trans-2,3-cis-3,4-dihydroxyproline and a dipeptide fragment of Mefp1 which contains this amino acid.

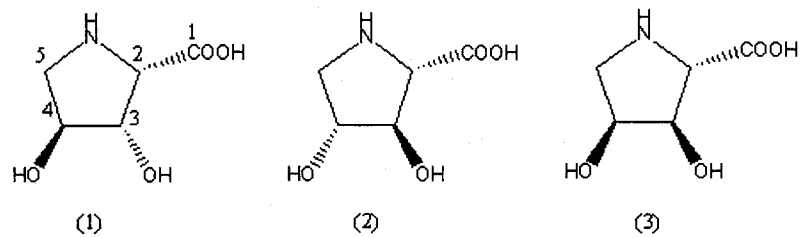


Figure 1.2.3 Naturally occurring 3,4-dihydroxyprolines.

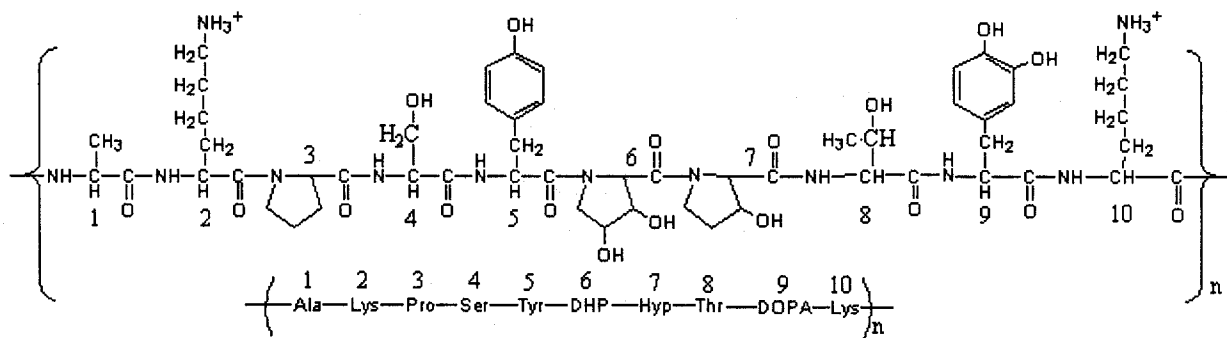


Figure 1.2.4 The repeating unit of decapeptide in the adhesive proteins Mefp1 (after [105]).

1.3 Rhamnogalacturonan II (RG-II) and Silicon's Influence on Plant Cell Walls

Although no evidence was found for the presence of organosilicate complexes in the bulk biofluids of wheat [50], the high concentration of silicon in the cell walls of higher plants would suggest that organosilicate species might well occur in association with macromolecular cell wall components. Coincidentally, most of the reported symptoms of Si-deficiency in plants (*e.g.*, lodging, pathogen susceptibility, *etc.*) [4] could be readily attributed to compromised cell-wall integrity. We therefore turned our

attention to the polysaccharides in the primary cell wall.

The primary wall, located between the middle lamella and the secondary wall, is composed of polysaccharides (pectin, cellulose and hemicellulose) and proteins. The term “pectin” encompasses a group of acidic heteropolysaccharides with distinct structural domains. Homogalacturonan (HGA), rhamnogalacturonan I (RG-I), and the substituted galacturonan referred to as rhamnogalacturonan II (RG-II) are the predominant pectic polysaccharides present in the primary cell walls [106]. RG-II is of particular interest here because it interacts with boron *in vivo* to form a 1:2 borate:diol ester (dRG-II-B; two RG-II chains joined by a single boron cross-link) and, in so doing, can dramatically alter the primary cell wall morphology [107].

First identified in 1978, RG-II is a structurally complex pectic polysaccharide containing 12 different glycosyl residues bound together by more than 20 different types of glycosyl linkages [108]. Some twenty years later it was discovered that most of the boron in plant cell walls exists in the form of dRG-II-B. The B-binding site on RG-II was later determined to be the OH-2 and OH-3 hydroxyls of the apiofuranosyl residue on side chain A [109; refer to Figure 3 in reference 93]. These findings led to the suggestion that boron is required by plants to cross-link cell wall pectic polysaccharides

[109,110] and thereby regulate the mechanical and biochemical properties of the cell wall [93]. Fleischer *et al.* [111] showed that the walls of growing B-deficient *Chenopodium album* cells contain RG-II, but not the boron cross-linked dimer. Upon addition of boron, RG-II rapidly converted to dRG-II-B and the wall pore size simultaneously decreased. Similar findings have been reported for a wide variety of other plant types [112-114]. Moreover, some workers [115,116] noted that boron deficiency in beans leads to a loss of hydroxyproline-rich proteins that are bound covalently to RG-II. This could indicate the occurrence of some connection of RG-II to proteins that may contribute to the strength and integrity of the wall [116]. Additionally, the dRG-II-B complex has been shown to have a strong affinity for selectively chelating heavy metals including lead, barium and strontium [107].

Monomeric and dimeric RG-II can be isolated directly from fermented fruit beverages such as cider and wine by ethanol-precipitation or ultrafiltration, and then purified by a combination of size-exclusion and ion-exchange chromatography [117-119]. Wines and fruit juice may contain between 50 and 400 mg/l of RG-II [107,119].

As early as 1992, germanium was reported to delay the symptoms of boron deficiency in plants and substitute for boron in suspension-cultured carrot cells [120].

Germanate cross-linked RG-II dimer (dRG-II-Ge) forms when monomeric RG-II reacts with germanic acid *in vitro* [121]. However, germanium does not rescue the growth and tissue strength of boron-deficient pumpkin plants [122]; dRG-II-Ge is less stable than its borate cross-linked counterpart because of differences in the geometry and coordination number at the germanate centre [121, 122].

Given the knowledge that boron and germanium transform the structure of plant cell walls by cross-linking pectic polysaccharides, it seems rather surprising that the literature contains no suggestion that silicon might play an analogous role. Silicon is far more abundant than either B or Ge – in both plant and soil – and indeed many of the benefits conferred by silicon on plant growth could conceivably be linked to an increase in cell wall integrity. Moreover, the apiofuranosyl binding site on RG-II has *vicinal cis*-diol functionality (as in ribose) that is favorable to binding silicon.

In the present study, we carried out a three-part investigation to determine if and how silicon interacts with cell wall polysaccharides: 1. We characterized silicon interaction with apiose, the active binding site of RG-II. 2. We attempted extraction of RG-II from red wine and searched for evidence of its interaction with aqueous silicon. 3. We studied the influence of Si-availability on cell wall structure in hydroponically

grown wheat.

1.4 Silicon Uptake and Excretion in Humans

Above, we presented evidence to suggest that silicon plays an important role in the formation of bone and connective tissue in animals. The dietary uptake of silicon from fluids [123-125, 66] and solid foods [126-128, 66] has been studied extensively. Recently, Powell and coworkers [123, 66] characterized the kinetics of silicon uptake and excretion in humans following the oral intake of orthosilicic acid. They found that the Si concentration in blood serum peaks at *ca.* 1 h and that most silicon is excreted in the urine within 6 h [65, 66]. However, the identity of the Si-containing molecule(s) in human biofluids was not determined.

A final goal of the present investigation was therefore to identify the major silicon-bearing molecules in human blood and urine.

1.5 Silicon-29 NMR

Nuclear magnetic resonance spectroscopy is one of the most powerful and versatile tools for examining chemical substances at the molecular level. Silicon-29 NMR is useful for investigating Si-containing molecules, but, owing to the isotope's low natural isotopic abundance (4.7%) and poor receptivity (12.7% that of ^1H), it is necessary to employ highly concentrated solutions, numerous transient acquisitions, and/or materials enriched in ^{29}Si . Additionally, ^{29}Si enrichment permits detection of ^{29}Si - ^{29}Si scalar coupling which is a potent source of structural information. In aqueous solution rapid inter- and intra-molecular ^1H - ^1H chemical exchange obscures all evidence of ^1H - ^{29}Si J -coupling involving hydroxy group protons, even down to the solution's freezing point. Nonetheless, information from three bond ^{29}Si -O-C- ^1H coupling can often be obtained [82, 83, 87]. It is essential to acquire ^1H -decoupled spectra with the decoupler channel gated off during the acquisition period in order to prevent nuclear Overhauser distortion, which is negative in the case of ^{29}Si NMR. Finally, the characteristically slow longitudinal (T_1) relaxation of ^{29}Si necessitates extremely long inter-pulse delays [129].

The possible chemical shift range for ^{29}Si NMR is about 200 ppm. For

silicates, three spectral regions are apparent and correspond, in order of decreasing frequency, to species containing tetraoxosilicon (*Q*-centres, *ca.* -70 to -105 ppm), pentaoxosilicon (*P*-centres; *ca.* -98 to -110 ppm) and hexaoxosilicon (*H*-centres; *ca.* -135 to -143 ppm) [82, 38, 85, 90(a)].

Chapter 2 – Experimental

2.1 General Sample Preparation

Type-I deionized/distilled water (DDW) used throughout this study was purified through “macropure”, “ultrapure” and “organic free” resin cartridges (Barnstead E-pure) and then filtered (0.2 μ m). The silicon concentrations of the purified DDW and of the deuterated water (D₂O) used to provide a field/frequency lock were below the ICP-AES (Varian Vista Pro Radial) detection limit of 0.02 μ g/L. All samples were prepared and stored in containers of low density polyethylene (LDPE), Teflon FEP or Teflon TFE. The only glassware used was the rotary evaporator employed for RG-II extraction. Plastic labware was cleaned by successively soaking in 10% nitric acid, 10% hydrochloric acid, 0.01 M Na₂H₂EDTA and, finally, DDW. Solutions were transferred using non-lubricated polypropylene syringes (Sigma-Aldrich) in conjunction with Teflon FEP needles and LDPE pipettes. The chemical reagents employed in this study are listed in Table 2.1.

Table 2.1 Chemical reagents employed in this study.

Reagent	Supplier / Purity	Molecular formula (F.W.; g/mol)
acetic acid (glacial)	Anachemia / 99.7%	CH ₃ COOH (60.05)
boric acid	Sigma-Aldrich / 99.995%	H ₃ BO ₃ (61.83)
deuterium oxide	Sigma-Aldrich / 99.9 atom% ² H	D ₂ O (20.03)
ethanol	Caledon / 95%	C ₂ H ₆ O (46.07)
hydrochloric acid	Caledon / 36.5-38.0%	HCl (36.46)
3-phenylphenol	Sigma-Aldrich / 90%	C ₁₂ H ₁₀ O (170.21)
potassium hydrogen phthalate	Sigma-Aldrich/ 99.95-100.05%	2-(HO ₂ C)C ₆ H ₄ CO ₂ K (204.23)
Sephadex ^(TM) G-75	Amersham	N/A
silicon-29 oxide (amorphous)	Isonics / (a) 70 atom% ²⁹ Si (b) 98.7 atom% ²⁹ Si (c) 99.35 atom% ²⁹ Si	SiO ₂ (a) (60.6949) (b) (60.9631) (c) (60.9692)
silicon tetrachloride	Sigma-Aldrich / 99.998%	SiCl ₄
sodium borate (crystalline)	Fisher / 100.2%	Na ₂ B ₄ O ₇ ·10H ₂ O (381.37)
sodium hydroxide	Sigma-Aldrich / 99.998%	NaOH (40.00)
sulfuric acid	Fisher / 95.0-98.0%	H ₂ SO ₄ (98.075)

Sodium hydroxide stock solutions were made by mixing high purity sodium hydroxide pellets with pre-boiled DDW, and then titrating against potassium hydrogen phthalate using 1% phenolphthalein indicator. Sodium silicate solutions were prepared by tumbling aqueous NaOH with freshly dried amorphous silica, prepared by hydrolysis of SiCl_4 , at 60 °C for 3-7 days. Silicon-29 enriched silicate solutions were prepared by dissolving commercial $^{29}\text{SiO}_2$ (amorphous, but with *ca.* 10 %wt cristobalite) in aqueous NaOH at 150 °C for 24-48 h using a PTFE-lined pressure vessel.

All pH measurements were performed at 25 °C using Phydrion Microfine pH paper when the solution volume was < 3 mL (minimum precision ± 0.3 pH unit), or an Orion ROSS glass combination pH electrode calibrated at pH 4.00, 7.00 and 11.00 prior to each use (precision ± 0.001 pH unit). Since samples which were prepared for NMR analysis were deuterated (*ca.* 10 atom% ^2H), the recorded values were actually a weighted combination of pH and pD (where $\text{pD} = \text{pH} + 0.4$ [130]) and thus included a small systematic error of *ca.* + 0.04 pH unit that was considered to be insignificant in the present context.

2.2 NMR Measurement

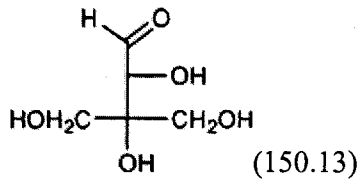
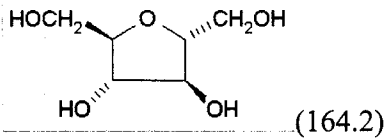
Silicon-29 NMR spectra were acquired on Varian Inova 500 (Lakehead University), Bruker AMX 500 (University of Manitoba) and Varian Inova 750 (Keck NMR Facility, University of Illinois at Urbana-Champaign) NMR spectrometers operating at 99.28, 99.31 and 149.00 MHz, respectively. Glass coil supports in the AMX 500 probe head were replaced with Vespel SP-1 polyimide components in order to eliminate ^{29}Si background signals. Chemical shifts are reported relative to tetramethylsilane, employing the orthosilicate monomer peak, set to -70.0 ppm, as a secondary reference. Carbon-13 and ^1H NMR spectra were obtained at 125.67 and 499.72 MHz, respectively, on the Varian Inova 500 spectrometer. Attention was paid to avoid sample contamination by contact with glass surfaces, and all samples were contained in custom-made 10mm Kel-F NMR tubes (9 mm I.D.) or Teflon FEP-lined glass NMR tubes (8 or 4 mm I.D.). The detailed spectral parameters are provided in the individual figure captions.

2.3 Speciation of Small Organosilicate Complexes

The interactions between aqueous alkaline silicate and (a) the 4-aminobutanol-

trypsin system, (b) DHP (2,3-*trans*-3,4-*cis*-3,4-dihydroxy-L-proline), (c) DHP-containing dipeptide Ac-Tyr-DHP-NHME (ATDN), (d) D-apiose, and (e) 2,5-anhydro-D-mannitol were examined separately under various solution conditions using ^{13}C and ^{29}Si NMR spectroscopy. Details of these organic ligands are listed in Table 2.2. Tables 2.3 and 2.4 present the experimental conditions employed in studies involving DHP and ATDN, respectively. Addition of NaOH to samples in Tables 2.3 and 2.4 eventually resulted in *ca.* 5% dilution, which was considered to be insignificant in the present context.

Table 2.2 Organic ligands employed in this study.

Reagent	Supplier	Molecular structure (F.W.; g/mol)
4-amino-1-butanol	Sigma-Aldrich (98%)	$\text{HO}(\text{CH}_2)_4\text{NH}_2$ (89.14)
trypsin (from porcine pancreas)	Sigma-Aldrich	type IX-S (<i>ca.</i> 23800)
D-apiose	Omicron (0.100 M)	 HOCH_2 (150.13)
2,5-anhydro-D-mannitol	Sigma-Aldrich	 (164.2)

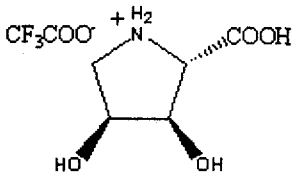
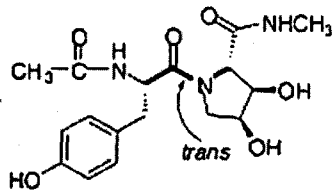
<p>2,3-<i>trans</i>-3,4-<i>cis</i>- 3,4-dihydroxy-L-proline</p>	<p>Dr. Carol M. Taylor (Massey University, New Zealand)</p>	 <p>(261.15)</p>
<p>Ac-Tyr-DHP-NHME</p>	<p>Dr. Carol M. Taylor (Massey University, New Zealand)</p>	 <p>(365.38)</p>

Table 2.3 The pH and NaOH content of DHP-containing silicate samples prepared by dissolving 87.7 mg DHP in 0.3610 g DDW and tumbling with 10.2 mg amorphous silica (98.7 atom% ^{29}Si) at 310 K. After each successive addition of NaOH, the sample pH was allowed to equilibrate before conducting ^{13}C and ^{29}Si NMR analysis.*

NaOH Content (mol kg ⁻¹)	Sample pH (±0.3)
0	5.3
0.174	7.9
0.373	7.9
0.551	7.9
0.770	7.9
0.956	7.9
1.218	7.9
1.485	9.8
1.733	10.1
2.021	11.1

2.238	11.7
2.589	13.3

* Amorphous silica was visible in each sample up to pH > 11.1.

Table 2.4 The pH and NaOH contents of ATDN-containing silicate samples prepared by dissolving 83.7 mg ATDN in 0.2910 g DDW and tumbling with 7.4 mg amorphous silica (98.7 atom% ²⁹Si) at 310 K. After each successive addition of NaOH the sample pH was allowed to equilibrate before conducting ¹³C and ²⁹Si NMR analysis.*

NaOH Content (mol kg ⁻¹)	Sample pH (±0.3)
0	4.0
0.251	8.8
0.496	10.8
0.767	11.1
1.151	12.0
1.419	12.3
1.739	13.0

* Amorphous silica was visible in each sample up to pH > 11.1.

2.4 Isolation and Purification of Red Wine RG-II

The following procedure is based on a RG-II purification scheme provided by Dr. Stefan Eberhard, Complex Carbohydrate Research Center, University of Georgia (2002, private communication). Several minor modifications have been made to the original procedure.

Two different wines were employed: Peller Estates Merlot 2002 (4 L), produced from grapes of various international origins; and Kittling Ridge Estates Merlot 2002 (7.5 L), produced from Ontario grapes (Grimsby Ridge, Niagara Escarpment). Sodium azide (0.02 g / 250 mL of wine) was added to retard the growth of bacteria. Each 1.2 L aliquot was concentrated to 1/5th the original volume on a rotary evaporator at 35-40 °C. After 200 mL of wine concentrate was accumulated, 340 mL 95% cold ethanol (4 °C) and 2.7 mL 36-38% HCl were added quickly, and the mixture kept at 4 °C for 24 h. The ethanolic mixture was then transferred into four 250 mL bottles and centrifuged for 30 min at 9000 rpm. The temperature throughout the centrifuging process was maintained at 0-4 °C. The solid pellets in each bottle were collected and washed with a mixture of 500 mL 95% ethanol and 2.5 mL 36-38% HCl under rough agitation. The solid/ethanol mixture was again centrifuged and the resulting pellets

were dissolved in 100 mL 0.2 M boric acid that was buffered at pH 3.3 (4 °C) with 50 mM potassium hydrogen phthalate/HCl. After 24 h, the mixture was dialyzed against DDW with 6000-8000 MWCO membrane (Spectra/Por 1) at 4 °C for at least 24 h. The dialysate was filtered using 0.45 µm (Durapore, HVLP) membrane filters and then concentrated down to 10 mL on a rotary evaporator at 35-40 °C.

The resulting RG-II concentrate was further purified through a Sephadex G-75 size exclusion chromatography (S.E.C.) column by elution with 50 mM pH 5.2 sodium acetate/acetic acid buffer with 0.02% sodium azide at a flow rate of 1 mL/min. The column eluant was collected into 120 15 mL tubes and the uronic acid content of each tube assayed by the m-phenylphenol method [131]. Fractions that possibly contained mono- or dimeric RG-II, as indicated by the uronic acid assay, were treated with 40 mL 0.1 M HCl for 1 h to release boron from the dimeric RG-II complex, and then dialyzed (2000 MWCO membrane, Spectra/Por 7) for 24-48 h against DDW to remove boron and other salts. Boron-11 NMR spectra were acquired before and after the HCl treatment. The resulting boron-free sample was then lyophilized from D₂O, yielding 50-200 mg of silver white solid with mushroom-like texture. The product was analyzed by ES-MS and NMR.

2.5 Effect of Silicon On Cell Wall Morphology of Wheat (*Triticum aestivum*)

Two sets of wheat plants were grown to maturity under previously described conditions [50, 132] at the University of California, Davis: one set in February 2004 and the other in June 2004. The freshly harvested plants were wrapped in tissue soaked with 0.50 mM CaSO₄ in order to prevent cell damage by desiccation or osmosis, and couriered to Thunder Bay in insulated containers.

The February set consisted of two plants grown in a nutrient medium containing 0.020 mM silicic acid (“+Si”), and two plants that were grown in a Si-free medium (“-Si”). In addition, short sections of stem from each of the -Si plants were soaked in a solution of 0.020 mM silicic acid and 0.50 mM CaSO₄ at pH 6.0 for 30 min before fixation (“-Si to +Si”).

i) Paraffin Sections. Three millimeter segments from the stem of each plant were fixed in FAA (90 mL 70% ethanol, 5 mL glacial acetic acid, 5 mL formalin) for several days before washing out in 50% ethanol. These were dehydrated and embedded in paraffin according to Johansen [133]. Sections were cut 9 μm thick, mounted and stained 2 h in Fast Green FCF (0.10% in 90% ethanol), rinsed in 95% ethanol, and then dehydrated in changes of 100% isopropanol before clearing in xylene and mounting in

Permout (Fisher).

ii) Plastic Sections. Additional stem segments from the February set of plants were processed for embedding in JB4-Plus plastic medium (Polysciences). Sections about 0.5 μm thick were stained 1 min in a solution of 0.5% Toluidene Blue O, 0.5 g borax and 100 mL distilled water, washed in water, dried and then mounted in Permout.

The paraffin and plastic sections were viewed under light microscope using a x100 oil immersion lens. Cell wall thickness was measured using an ocular graticule. Paraffin sections were also mounted for SEM analysis. Sections 20 μm thick were floated on water containing two drops of glycerin albumen (Fisher) per 50 mL of distilled water, deposited on a SEM stub, and dried at *ca.* 53 °C overnight. The paraffin was removed by rinsing the stub with three changes of xylene and three changes of hexamethyldisilazane, each change lasting about 5 min. The last solution upon drying does not produce distorting surface tension effects. The affixed sections were gold-coated and examined with a JEOL 5900 LV SEM operated at 10 kV, with a spot size of 22 μm and a 11 mm working distance.

The June set of wheat plants consisted of two plants grown in a nutrient medium containing 0.020 mM silicic acid (“+Si”), two plants that were grown in a Si-free

medium (“-Si”), and, this time, two plants that were grown Si-free but were exposed to the medium containing 0.020 mM silicic acid and 0.50 mM CaSO₄ for 60 min before harvesting (“-Si to +Si”). Paraffin embedded stem sections were prepared for SEM analysis using the method described above.

Cell wall thickness was measured using both optical microscopy and SEM, and using only cell walls that were perpendicular to the field of view. Cell wall tilt is the largest potential source of inaccuracy although, as shown in Figure 2.5.1, angles $\leq 20^\circ$ yield relatively little error. Fortunately, the tilt angle is readily apparent in the 20 μm sections used for SEM analysis. Optical microscopy measurements were correct to about $\pm 0.25 \mu\text{m}$, whereas the SEM values were $\pm 0.12 \mu\text{m}$.

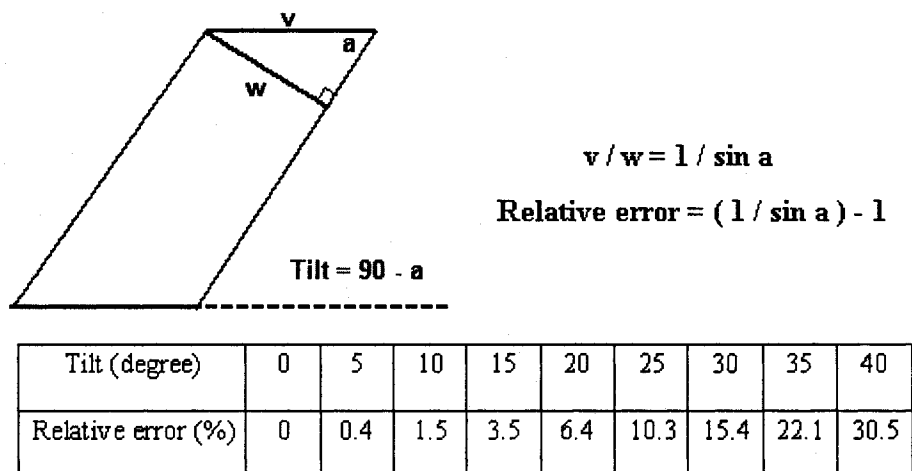


Figure 2.5.1. Relative error in cell wall thickness resulting from tilt angle.

Representative stem, leaf and flower samples from the June plants were digested and analyzed by ICP-AES, employing EPA Method 3051A [134]. Ground, oven-dry tissue was combined with concentrated nitric and hydrochloric acids (trace metal grade, Fisher) and digested at 175 °C for 30 min in a CEM Mars 5 microwave oven using closed Teflon vessels (CEM XP-1500 Plus). The brown fumes in each vessel were cleared by addition of 1 mL 30% hydrogen peroxide (Fisher), and the resulting clear samples diluted to 50 mL with DDW and analyzed on a Varian Vista Pro ICAP Radial spectrophotometer.

2.6 Analysis of Silicon Uptake and Excretion in Humans

The following procedure was reviewed and approved by the Lakehead University in accordance with the guidelines set out in the *Tri-Council Policy Statement: Ethical Conduct for Research Involving Humans* [135].

A healthy, 20 year old male volunteer (1.83 m, 77 kg) with normal renal function (serum creatinine level of 100.0) was recruited from the Department of Chemistry, Lakehead University. Details of the study were explained to the volunteer and a written consent form signed by him prior to starting the study.

After fasting overnight for 11 h, the subject voided his bladder and urine was collected for 3 h in a pre-weighed LDPE container for measurement of baseline silicon excretion. The subject ingested 500 mL of type-I water over the 3 h period, but otherwise remained fasted. Thereafter, the subject renewed his normal eating habit except for the complete avoidance of high silicon-containing foods (beer, bread, cereals, rice, bananas, string beans and raisins).

After again fasting overnight for 11 h, the subject voided his bladder and had 10 mL blood collected from a forearm vein to provide a baseline serum silicon measurement. The subject then ingested 500 mL type-I water that contained 2.87×10^{-3} mol kg⁻¹ SiO₂ (41.5 mg; 98.7 atom% ²⁹Si) and 3.03×10^{-3} mol kg⁻¹ NaOH at pH = 7.9 ± 0.3. Additional blood samples (10 mL) were collected after 0.5, 1.0, 1.5, 2.0, 3.0, 4.0, 5.0 and 6.0 h. A second 10 mL blood sample was collected at the 1.5 h mark to ensure that there was enough sample for NMR analysis. Urine was collected in two 3 h fractions (*i.e.*, 0-3 h and 3-6 h) in separate pre-weighed LDPE bottles. The subject remained fasted except for the ingestion of 500 mL type-I water over the last 3 h of the sampling period (3-6 h).

All blood samples were taken by a certified phlebotomist using sterile,

silicon-free 10 mL polypropylene syringes and 22 G stainless steel needles (Sigma Aldrich). The blood was transferred to polypropylene centrifuge tubes (Nalgene), allowed to clot at room temperature for 1 h, and then separated by centrifugation (9000 rpm) at room temperature for 10 min. The resulting serum was transferred to LDPE bottles and stored at ambient temperature until analysis.

ICP-OES analysis (Jobin-Yvon JY24) was performed at St. Thomas' Hospital, London, UK. Serum and urine samples were diluted 1:4 and 1:1, respectively, with 0.26% nitric acid and stored at *ca.* 4 °C. The Si concentration was measured at 251.611 nm with an integration time of 1 s for serum and 0.5 s for urine at a sample flow rate of 1 mL min⁻¹. Silicon-29 NMR analysis was conducted at the University of Illinois at Urbana-Champaign (Varian Inova 750), each sample aliquot being diluted 10% with D₂O to provide a field/frequency lock. Afterwards, the serum and urine samples were destroyed.

Chapter 3 – Results and Discussion

3.1 NMR examination of the 4-aminobutanol-trypsin-silicate system

As discussed in Chapter 1, alkaline aqueous solutions containing borate, trypsin and 4-aminobutanol yield a stable ternary complex in which the boron centre is coordinated to the hydroxymethyl group on serine-195 of trypsin and the oxygen atom of 4-aminobutanol [96, 97]. The formation mechanism for this complex is remarkably similar to that proposed by Zhou *et al.* [35] to account for silicatein's enzymatic role in the hydrolysis of organosilicon substrates, the active sites of silicatein α being residues of serine and histidine. Because boron and silicon exhibit somewhat similar complexing tendencies in alkaline solution, the 4-aminobutanol-trypsin-silicate system was used as a model for testing the proposed silicatein-mediated silicification mechanism.

Silicon-29 NMR spectra of a sample with $0.043 \text{ mol kg}^{-1} \text{ SiO}_2$ (70.0 atom% ^{29}Si), $0.21 \text{ mol kg}^{-1} \text{ NaOH}$, 0.22 mol kg^{-1} 4-aminobutanol and 6.1 mmol kg^{-1} trypsin contained signals from -70 to -98 ppm (with -70 ppm set to the $\text{Si}(\text{OH})_4$ peak), corresponding only to 4-coordinated silicate oligomers. No signals were apparent (within the detection limit of $0.12 \text{ mmol kg}^{-1}$) that could be associated with organosilicate

complexes containing 4-, 5- or 6-coordinated silicon.

The fact that silicon, unlike boron, is unable to bind with the histidine and serine residues of trypsin is not entirely surprising given our present understanding of organosilicate complexation in aqueous media. As previously discussed, aqueous boron is complexed by a wider variety of polyhydroxy molecules than silicon. It interacts with most 1,2- and 1,3-diols, and does so under acidic as well as basic conditions. Aqueous silicates, on the other hand, bind only to polyols with highly specific hydroxy group configurations [82-88]. (Silicon in fact binds covalently with many simple alcohols, but only to a limited extent and under *extremely* alkaline conditions [136].) The covalent interaction between silicatein and aqueous silicon proposed by Zhou *et al.* [35] seems unlikely, therefore, especially under near-neutral conditions. However, this finding by no means precludes the possibility that such amino acid residues play an active role in the hydrolysis of silicate or silicone compounds by virtue of some other type of interaction such as hydrogen bonding or electrostatic association [94].

3.2 Aqueous silicon interactions with 2,3-*trans*-3,4-*cis*-3,4-dihydroxy-L-proline

(DHP)

Several studies have shown that furanoidic molecules possessing vicinal *cis*-diol functionality are capable of hypercoordinating with silicon [87, 88, 90(a)]. One of the dominant features of the ^{29}Si NMR spectra of solutions containing such organosilicate complexes is the presence of three strong signals in the pentaoxosilicon region of the spectrum, between *ca.* -96 and -101 ppm. These three signals occur over a wide range of solution conditions and result from three different organosilicate species which are diastereomers of the monomeric *bis*(diolato)-hydroxo complex, $[(\text{L}=\text{O})_2\text{SiOH}]^-$ (where L represents the *cis*-diol ligand), each with a pentacoordinated silicon centre and a 2:1 ligand-to-Si ratio [88, 90(a)]. The amino acid 2,3-*trans*-3,4-*cis*-3,4-dihydroxy-L-proline (DHP) is structurally analogous to the furanoidic *cis*-diols and is expected to show similar Si binding affinity. Here we present the results obtained from a series of experiments.

DHP-complexation under alkaline conditions. As shown in Figure 3.2.1 (I), addition of 2,3-*trans*-3,4-*cis*-3,4-dihydroxy-L-proline to an alkaline silicate solution containing $0.443 \text{ mol kg}^{-1} \text{ SiO}_2$ and $1.545 \text{ mol kg}^{-1} \text{ NaOH}$ resulted in the appearance of

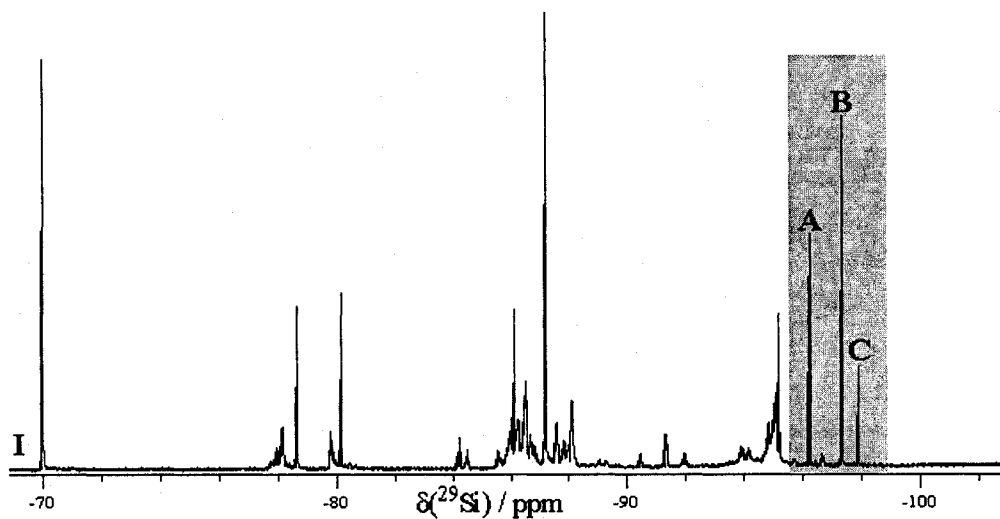
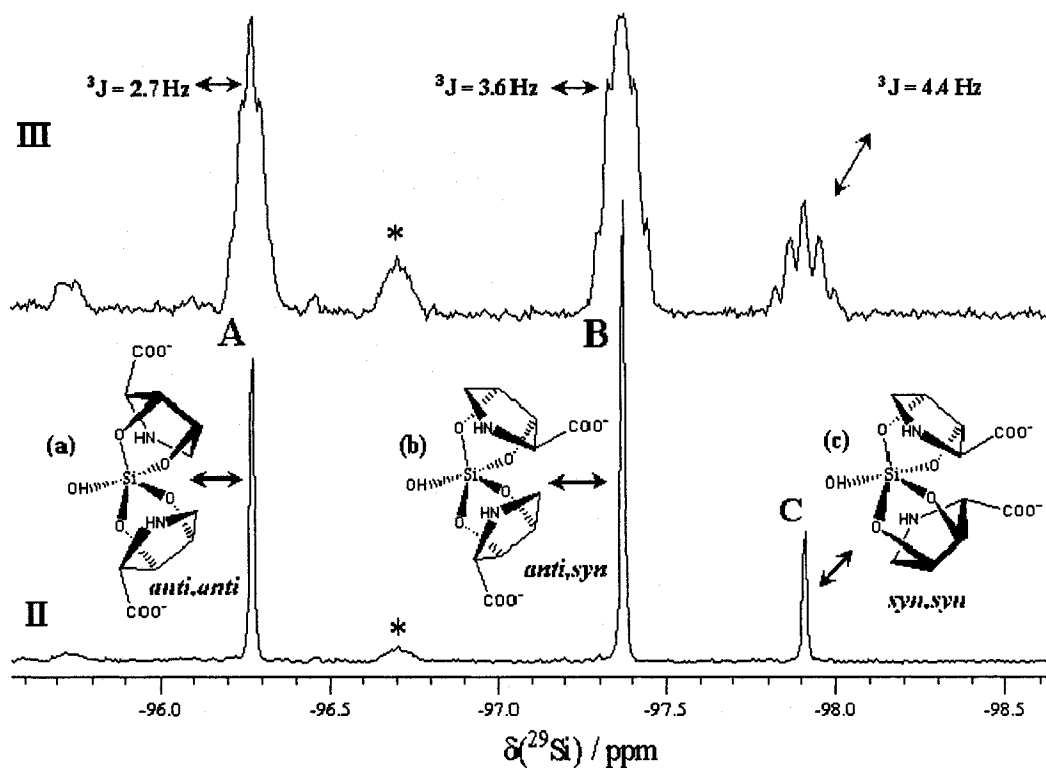


Figure 3.2.1 (I) Silicon-29 NMR (99.28 MHz) spectrum of an aqueous solution (pH=12.5) containing $0.891 \text{ mol kg}^{-1}$ DHP, $0.443 \text{ mol kg}^{-1}$ SiO_2 (70 atom% ^{29}Si) and $1.545 \text{ mol kg}^{-1}$ NaOH, recorded at 271 K using 1100 $\pi/2$ pulses, a 60 s inter pulse delay and gated ^1H -decoupling. (II) Expansion of the highlighted region in (I). (III) The equivalent spectrum acquired without ^1H -decoupling. The peak marked with * exhibits no ^{29}Si - ^1H scalar coupling and corresponds to non-complexed silicate species (species 18 in ref 137). This sample is more concentrated than those samples listed in Tables 2.3 and 2.4.

three strong ^{29}Si NMR signals in the pentaoxosilicon region at -96.28 (peak A), -97.38 (peak B) and -97.92 ppm (peak C). No peaks were observed in the hexaoxosilicon region (-135 to -143 ppm).

None of the three pentaoxosilicon signals exhibits ^{29}Si - ^{29}Si scalar J-coupling when solutions are enriched in ^{29}Si , suggesting that if the corresponding species contain more than one Si centre they are either magnetically equivalent or else separated by >4 bonds. Figure 3.2.1 (III) reveals that ^1H - ^{29}Si coupling splits each signal into a perfect pentet, with J-coupling = 2.7 (peak A), 3.6 (peak B) and 4.4 Hz (peak C). Since rapid ^1H - ^1H chemical exchange with water prevents detection of ^{29}Si -O- ^1H coupling, the observed pentets must instead arise from ^{29}Si -O-C- ^1H interactions involving protons on the five-membered ring of DHP. The 2.7 to 4.4 Hz splitting is indeed consistent with 3-bond (3J) scalar coupling. The silicon in each complex is thus bound to two hydroxy group oxygens on each of two DHP rings.

The chemical shifts and relative intensities of the three pentaoxosilicon peaks are similar to those recorded for silicate solutions containing furanoidic vicinal *cis*-diol molecules structurally related to DHP such as 1,4-anhydroerythritol [87, 88, 90(a)]. Accordingly, the peaks are assigned to three diastereomers of the monomeric

bis(diolato)-hydroxo complex $[(\text{DHP})_2\text{SiOH}]^-$ shown in Figure 3.2.1: (a) the *anti,anti* complex in which both DHP rings are facing away from the Si centre; (b) the *anti,syn* complex which has one ligand facing towards Si and the other facing away; and (c) the *syn,syn* complex in which both rings are oriented inwards towards silicon.

Molecular modeling calculations (MM2 energy minimization using *Chem3D* v.7.0) indicates that the Si-O-C-H dihedral angle is approximately 133.5° for the *syn,syn* complex and 98.4° for the *anti/anti* complex. Therefore, in accordance with the Karplus curve for the dependence of vicinal coupling on dihedral angle [138], the *syn,syn* complex should exhibit greater 3J coupling than the *anti/anti* complex. Thus, peaks A, B and C of Figure 3.2.1 can reasonably be expected to correspond to the *anti/anti*, *syn,anti* and *syn,syn* complexes, respectively. The same pattern of peak assignments likely holds for the pentaoxo Si complexes formed with furanoidic vicinal *cis*-diols [87,88; refer to Figure 1b in ref 88]. However, the high resolution of $^3J(^{29}\text{Si}-\text{O}-\text{C}-^1\text{H})$ coupling obtained here for the Si-DHP complexes indicates that they are much less labile (*i.e.*, undergo slower intermolecular Si-Si exchange) than the complexes formed by *cis*-1,2-dihydroxycyclopentane or furanoidic *cis*-diols such as ribose [87,88].

Figure 3.2.2 shows the ^{13}C NMR spectrum of a DHP solution before and after

the addition of sodium silicate. Peaks 6 and 7 of spectra (I) and (II) are attributable to the trifluoroacetate counterion used in the synthesis of DHP; these peaks were observable throughout the study and their relative intensities remained unchanged. The highlighted regions in spectrum (III) are assigned to DHP that is complexed to Si.

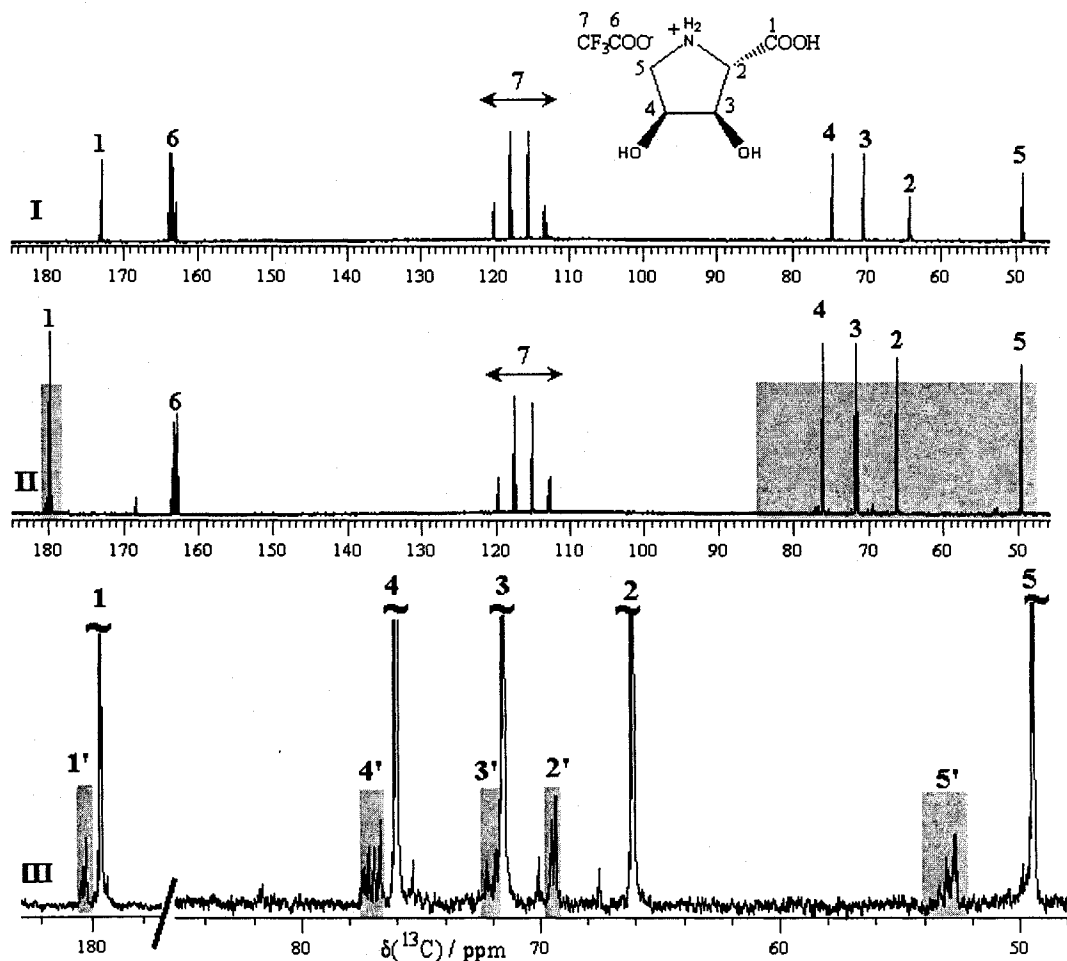
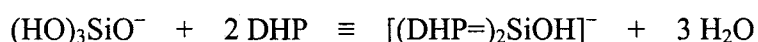


Figure 3.2.2 Carbon-13 NMR (125.66 MHz) spectra of the aqueous solutions containing: (I) 0.930 mol kg⁻¹ DHP (pH=5.3); and (II) 0.891 mol kg⁻¹ DHP, 0.443 mol kg⁻¹ SiO₂ (70 atom% ²⁹Si) and 1.545 mol kg⁻¹ NaOH (pH=12.5). Spectra were recorded at 271 K using 6000 π/2 pulses and a 10 s inter-pulse delay. ¹³C chemical shifts are recorded relative to TMS. Spectrum (III) shows the vertical expansion of the highlighted regions in (II). Peaks are labelled in accordance with the corresponding molecular sites, with peaks 1'-5' corresponding to the Si-DHP complexes. Sample (II) is more concentrated than sample (I).

These assignments are consistent with those reported for Si-complexes of *cis*-1,2-dihydroxycyclopentane and 1,4-anhydroerythritol [87, 88]; *i.e.*, Si coordination causes ligand ^{13}C signals to shift 1-4 ppm up frequency, with those corresponding to the Si-O-C linkage itself (C3 and C4 of DHP) being the least shifted. Comparison of the integrated peak areas with those of the corresponding ^{29}Si spectrum (Figure 3.2.1) indicates that the concentration of Si-coordinated DHP molecules is roughly twice the aqueous pentaoxosilicon concentration. Approximately 9.2% of the dissolved silicon in this particular solution is complexed by DHP.

If we equate all activity constants to unity and $[(\text{HO})_3\text{SiO}^-]$ to the silicate monomer (Q^0) concentration, the equilibrium constant for the complexation reaction



can be estimated as

$$K = \frac{[(\text{DHP}=\text{O})_2\text{SiOH}]^-}{[(\text{HO})_3\text{SiO}^-] [\text{DHP}]^2}$$

The resulting complexation constants are listed in Table 3.2.1 and, as had been indicated by the well-resolved $^3J(^{29}\text{Si}-\text{O}-\text{C}-^1\text{H})$ coupling, they reveal that the Si-DHP complexes are slightly more stable than other Si-polyolate species under similar solution conditions.

Table 3.2.1 Characterization of pentaoxosilicon DHP complexes in solution containing 0.44 mol kg⁻¹ SiO₂, 1.55 mol kg⁻¹ NaOH and 0.89 mol kg⁻¹ DHP at 271 K. (Refer to the spectrum and species depicted in Figure 3.2.1(II).)

Si species [(DHP=) ₂ SiOH] ⁻	$\delta(^{29}\text{Si})$ /ppm ^a	³ J (²⁹ Si-O-C- ¹ H) /Hz	Average Si-O-C-H dihedral angle ^b	Concentration /mol kg ⁻¹	K ^c
<i>anti,anti</i> (a)	-96.280	2.7	98.4°	0.0147	0.65
<i>syn,anti</i> (b)	-97.382	3.6	134.3° 97.4° (<i>syn</i>) (<i>anti</i>)	0.0197	0.87
<i>syn,syn</i> (c)	-97.922	4.4	133.5°	0.0062	0.27

^a Silicon-29 chemical shifts are relative to TMS, using the silicate monomer peak at -70.0

ppm as a secondary reference. ^b Dihedral angles of each Si-O-C-H fragment are

estimated using *Chem3D* molecular modelling software (v. 7.0). ^c Relative uncertainty of equilibrium constants is ≤ 10%.

DHP-complexation under varied pH conditions. DHP is hence the first

amino acid shown to have Si binding affinity, albeit only in alkaline solution. Our next step was to determine its binding affinity under pH conditions that are more biologically relevant.

Amorphous silica was tumbled in 0.93 mol kg⁻¹ DHP at 310 K for several

months. Each week, after monitoring the solution chemistry by ^{13}C and ^{29}Si NMR, the pH was raised incrementally by the addition of concentrated $\text{NaOH}_{(\text{aq})}$. Figure 3.2.3 shows the resulting ^{29}Si NMR spectra.

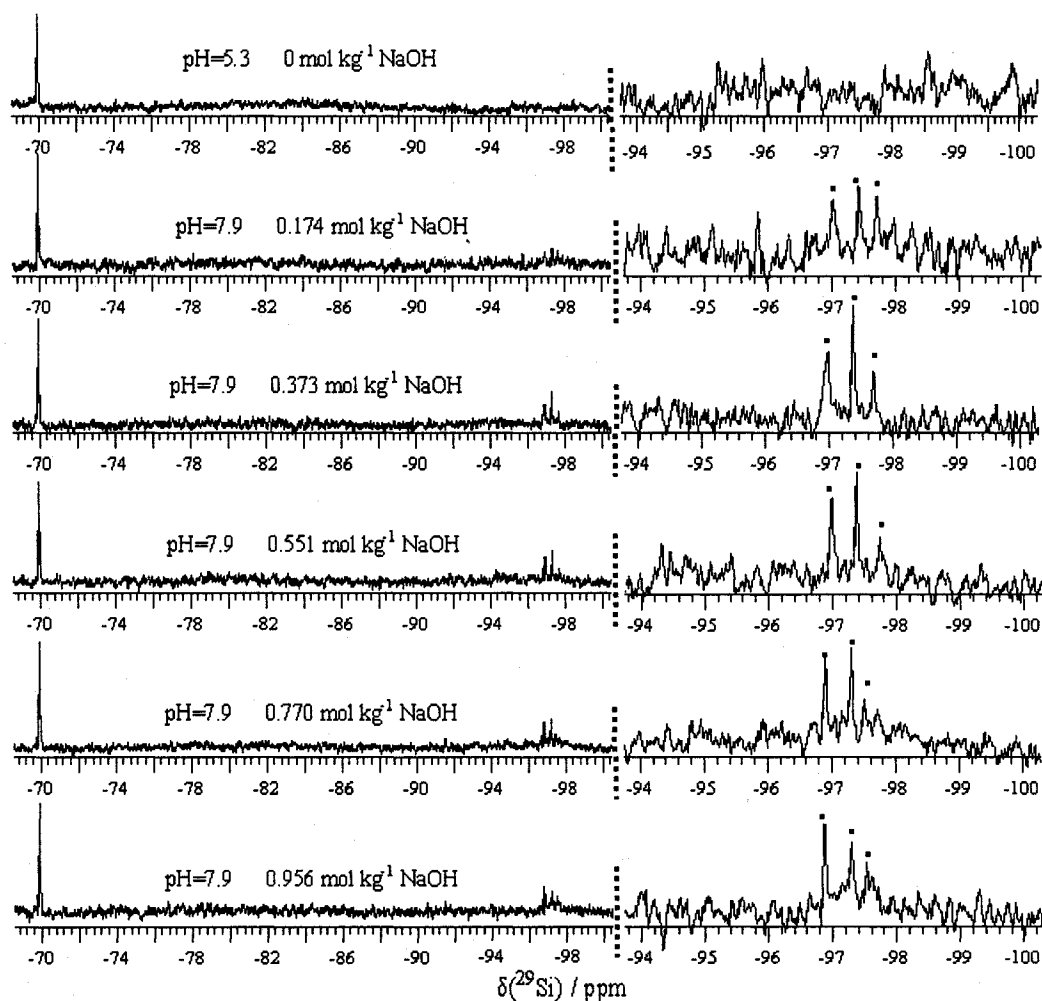


Figure 3.2.3(a) Silicon-29 NMR (99.28 MHz) spectra of the $0.930 \text{ mol kg}^{-1}$ 2,3-*trans*-3,4-*cis*-3,4-dihydroxyproline solution containing 10.2 mg amorphous silica (98.7 atom% ^{29}Si), 0.3610 g DDW and successively increased NaOH content (marked on each spectrum), recorded at 271 K using 1100-3000 $\pi/2$ pulses, a 60 s inter pulse delay and gated ^1H -decoupling. Artificial line broadening = 1.0 Hz. The vertically and horizontally expanded pentaoxosilicon spectral region is shown to the right. (No peaks were detected in the hexaoxosilicon region.) Peaks marked with • correspond to pentaoxosilicon complexes, and exhibit ^{29}Si - ^1H scalar coupling when the decoupler is switched off.

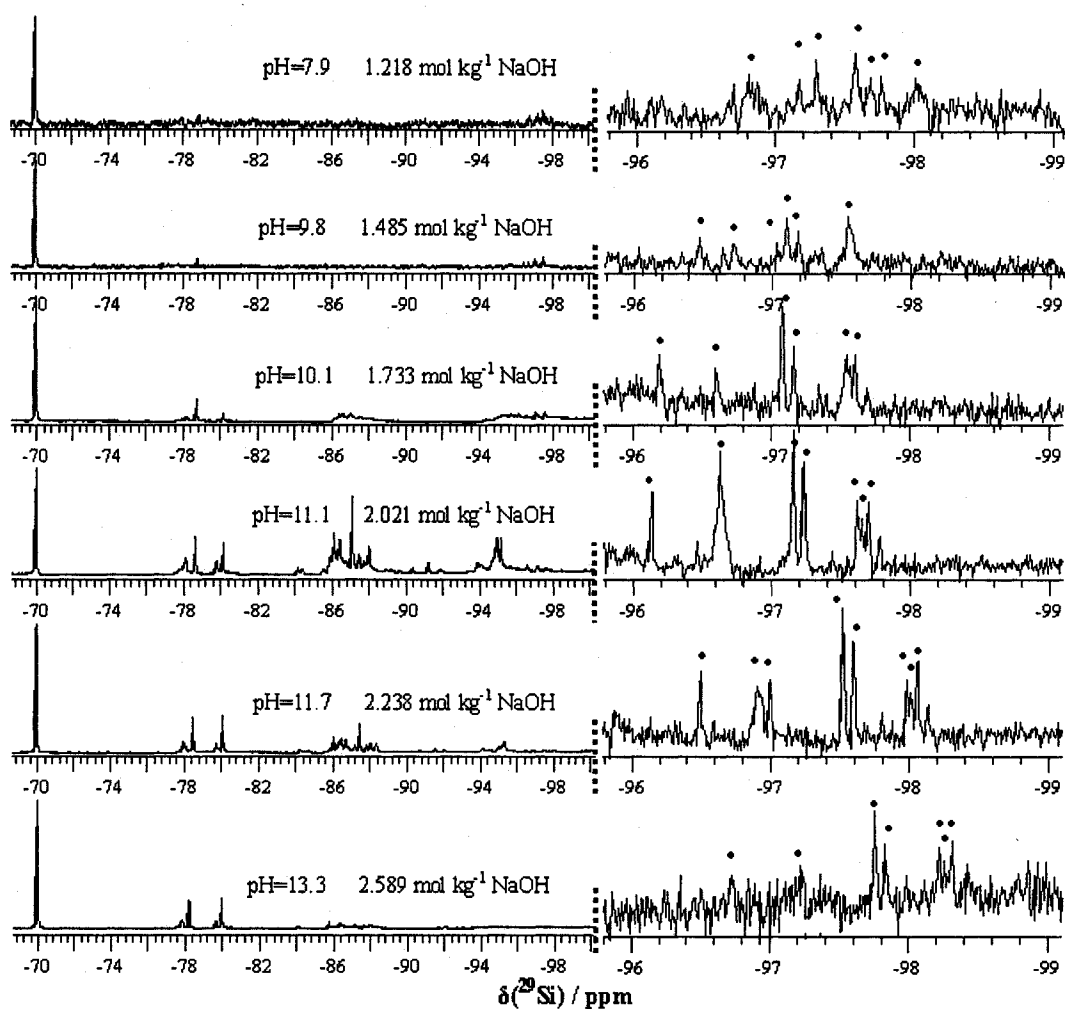


Figure 3.2.3(b) Continuation of figure 3.2.3(a)

The concentrated DHP was effective at buffering the reaction system, maintaining $\text{pH} \approx 7.9\text{-}8.1$ over a wide range of NaOH addition. It is noteworthy that only the resonances corresponding to monosilicic acid peak and the three pentaoxo Si-DHP complexes were observed over this pH range, and that the Si-DHP complexes account for as much as 52% of the dissolved silicon. Thus, DHP does indeed complex

silicon at biologically relevant pH conditions and to a very appreciable extent.

Once the buffer capacity of the DHP was exceeded, allowing pH to increase above 7.9-8.1, at least four new pentaoxosilicon ^{29}Si resonances appeared as shown in Figure 3.2.3(b). Carbon-13 NMR spectra revealed a simultaneous onset of DHP decomposition, indicating that the additional ^{29}Si peaks correspond to complexes formed between silicon and the DHP alteration products.

Complexation by DHP-containing dipeptide. A parallel experiment was conducted in which amorphous silica was tumbled at 310 K with a $0.787 \text{ mol kg}^{-1}$ solution of the DHP-containing dipeptide, Ac-Tyr-DHP-NHMe (ATDN). Again, pH was raised at one-week intervals by the addition of concentrated sodium hydroxide. Due to the absence of an amino or carboxyl terminus on ATDN, it exhibited none of the buffering effect observed for DHP. Figure 3.2.4 shows the resulting series of ^{29}Si NMR spectra.

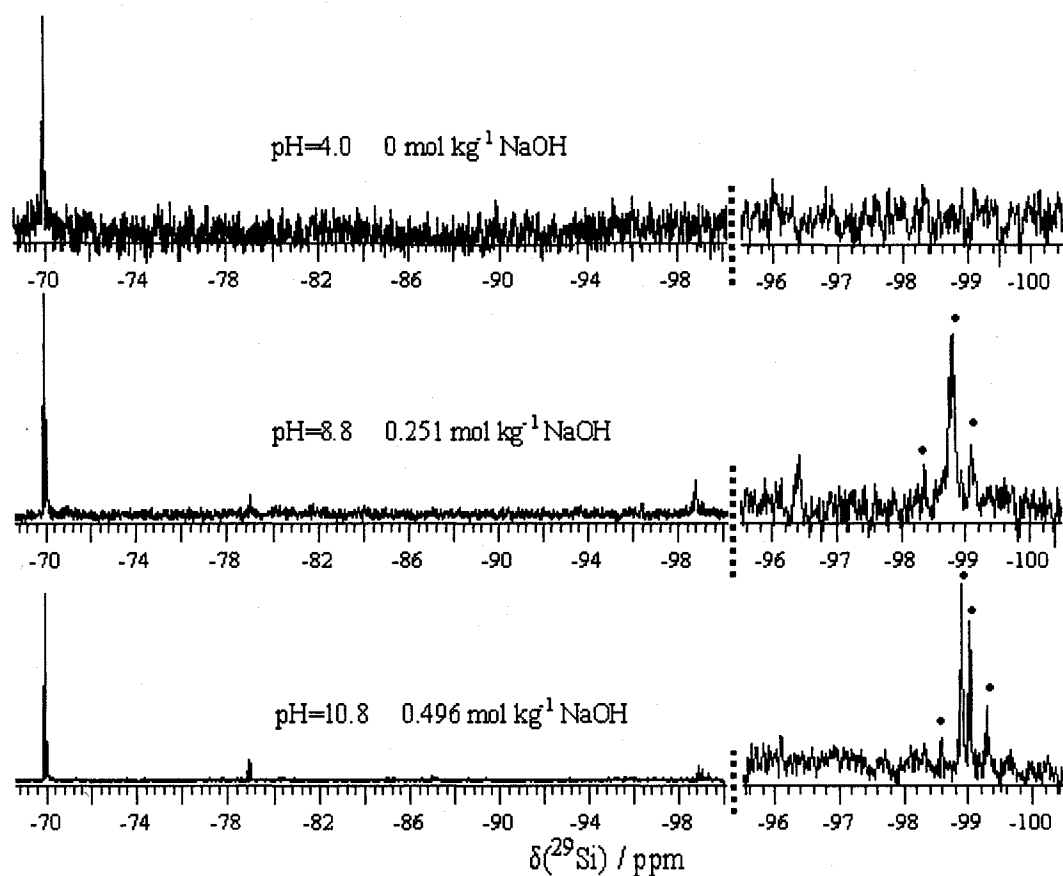


Figure 3.2.4(a) Silicon-29 NMR (99.28 MHz) spectra of $0.787 \text{ mol kg}^{-1}$ Ac-Tyr-DHP-NHMe (ATDN) solution containing 7.4 mg amorphous silica ($98.7 \text{ atom}\% \text{ }^{29}\text{Si}$), 0.2910 g DDW and successively increased NaOH content (marked on each spectrum), recorded at 271 K using $1100\text{-}3000 \pi/2$ pulses, a 60 s inter-pulse delay and gated ^1H -decoupling. Artificial line broadening = 1.0 Hz . The vertically and horizontally expanded pentaoxosilicon spectral region is shown to the right. (No peaks were detected in the hexaoxosilicon region.) Peaks marked with • correspond to pentaoxosilicon complexes, and exhibit ^{29}Si - ^1H scalar coupling when the decoupler is switched off.

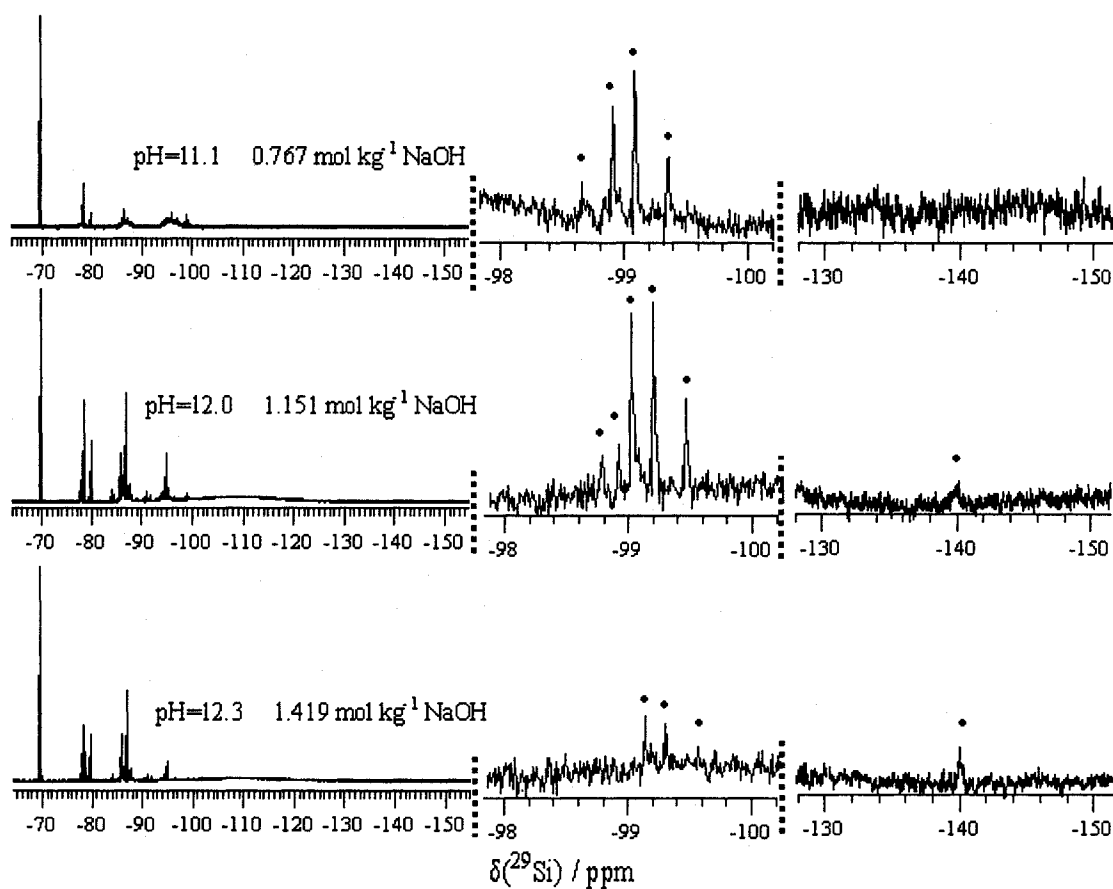


Figure 3.2.4(b) Continuation of figure 3.2.4(a) at progressively higher alkalinities. The pentaoxosilicon and hexaoxosilicon spectral regions are vertically and horizontally expanded and shown to the right.

ATDN also forms pentaoxosilicon species with aqueous silicon under near-neutral conditions, as evidenced by the presence of three pentaoxosilicon ^{29}Si NMR signals at pH 8.8. The chemical shift and height distribution of the peaks clearly indicate that the 2,3-*trans*-3,4-*cis*-3,4-dihydroxy-L-proline (DHP) residue is the active site of Si coordination, indicating a possible means by which the adhesive protein Mefp1

strongly binds to silicate surfaces in turbulent seawater.

Hexaaxosilicon complexes were detected in the ATDN sample at pH 12.0-12.3, as indicated by ^{29}Si peaks at *ca.* -140 ppm in Figure 3.2.4(b). The peaks are broad, indicating that the complexes undergo relatively rapid Si-Si chemical exchange with other solution species. Carbon-13 NMR spectra reveal progressive decomposition of the dipeptide as pH was raised to these levels, which would suggest that the hexaaxosilicon complexes might involve ATDN alteration products. Further work is required to characterize the decomposition of both DHP and ATDN, along with the nature of the resulting Si complexes.

This study provides the first ever evidence that the amino acid 2,3-*trans*-3,4-*cis*-3,4-dihydroxy-L-proline, whether existing freely or within an oligopeptide, spontaneously binds aqueous silicon to yield stable, hypercoordinated Si complexes. Moreover, the Si-binding tendency of DHP is the highest of all chelating ligands so far investigated under biologically relevant conditions of pH and Si concentration [84].

It is possible that 2,3-*trans*-3,4-*cis*-3,4-dihydroxy-L-proline (and perhaps also 2,3-*cis*-3,4-*cis*-3,4-dihydroxy-L-proline, the other *cis*-3,4-dihydroxy isomer of DHP) is

not nearly as rare as it is now thought to be. The only known occurrence of the amino acid at present is in *Mytilus edulis* foot protein 1 (Mefp1) where, originally, it had been misidentified as *trans*-3-hydroxyproline owing to the fact that the two amino acids species give nearly identical elution times on most analyzers [139]. Other logical places to look, therefore, include the hydroxyproline-rich structural glycoproteins found in both mammals (collagen is especially important [140]) and plants (speculated to be responsible for cross-linking pectic polysaccharides in the primary cell wall [115,116]), as well as the silica-precipitating proteins extracted from sponges and diatoms (*e.g.*, silaffins). Silicon interactions with *cis*-3,4-dihydroxy-L-proline might well account for the unexplained chemical role that silicon plays in all such environments.

3.3 NMR examination of D-apiose in alkaline silicate solution

Since most reported symptoms of Si-deficiency in plants (including increased susceptibility to lodging, fungal diseases, *etc.*) could conceivably be linked to diminished cell wall integrity, a likely place to seek evidence of organosilicate complexation in plants would be the cell wall. One possible binding site could be the hydroxyproline-rich glycoproteins mentioned above. Another is the pectic

polysaccharide rhamnogalacturonan-II (RG-II), which has been shown to form a 1:2 borate-RG-II diester complex in plant cell walls and, in so doing, help regulate their mechanical and biochemical properties [93,109,111]. Boron binds to RG-II at the *cis*-2,3-dihydroxy groups of an apiofuranosyl residue located on side-chain A of the polysaccharide [109]. The first step towards determining whether silicon plays a role in plants similar to that of boron is to establish whether it is complexed by apiofuranose as readily as it is by other furanoidic *cis*-diols such as ribose [87].

In aqueous solution, acyclic D-apiose is in equilibrium with four furanoidic isomers, of which three (B, C and D in Figure 3.3.1) have *cis*-dihydroxy functionality. One isomer (C) has three hydroxy groups in *cis*-1,2,3 configuration, thus providing not one but two possible Si binding sites and opening the door to the existence of a wide variety of organosilicate complexes.

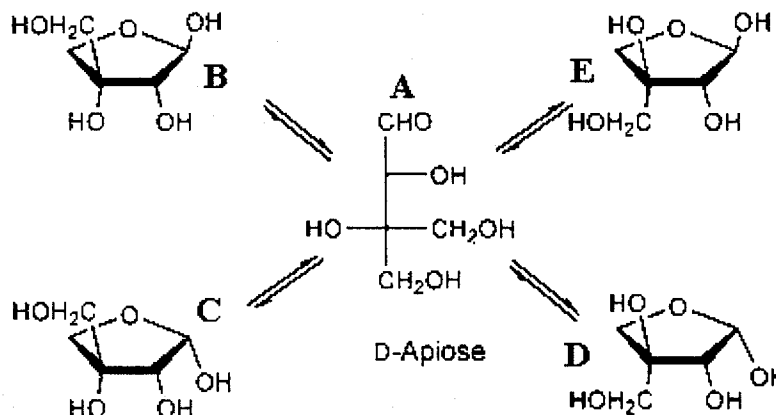


Figure 3.3.1 Possible molecular forms of D-apiose in aqueous solution.

We show in Figure 3.3.2(I) the ^{29}Si NMR spectrum of a sodium silicate solution to which a small amount ($0.087 \text{ mol kg}^{-1}$) of D-apiose was added. At least 7 pentaoxosilicon and 20 hexaoxosilicon resonances appear in the corresponding spectral regions, indicating the spontaneous formation of a great variety of organosilicate species. When the ^1H -decoupler is switched off, every pentaoxo- and hexaoxosilicon peak is transformed into a poorly resolved multiplet owing to $^3J(^{29}\text{Si}-\text{O}-\text{C}-^1\text{H})$ coupling within the complexes. The rate of Si-Si exchange at 278 K is just fast enough to obscure the anticipated 2-5 Hz 3J scalar coupling, and yet not broaden the ^1H -decoupled ^{29}Si resonances. The average lifetime of each organosilicate complex is thus somewhere between 0.05 and 0.5 s at this temperature.

Increasing solution alkalinity strongly disfavours the formation of apiose-derived organosilicate species, as indicated in Figure 3.3.2. The reason is apparent from the corresponding ^{13}C NMR spectra shown in Figure 3.3.3. Spectrum (I) is the ^{13}C NMR spectrum of pure D-apiose dissolved in water. The absence of carbonyl peaks at *ca.* 170-180 ppm and the presence of anomeric carbon peaks at *ca.* 95-105 ppm indicate that apiose exists exclusively in its furanoidic forms (within spectral detection limits). When pH is raised the rate of ring opening and closing increases sharply, as

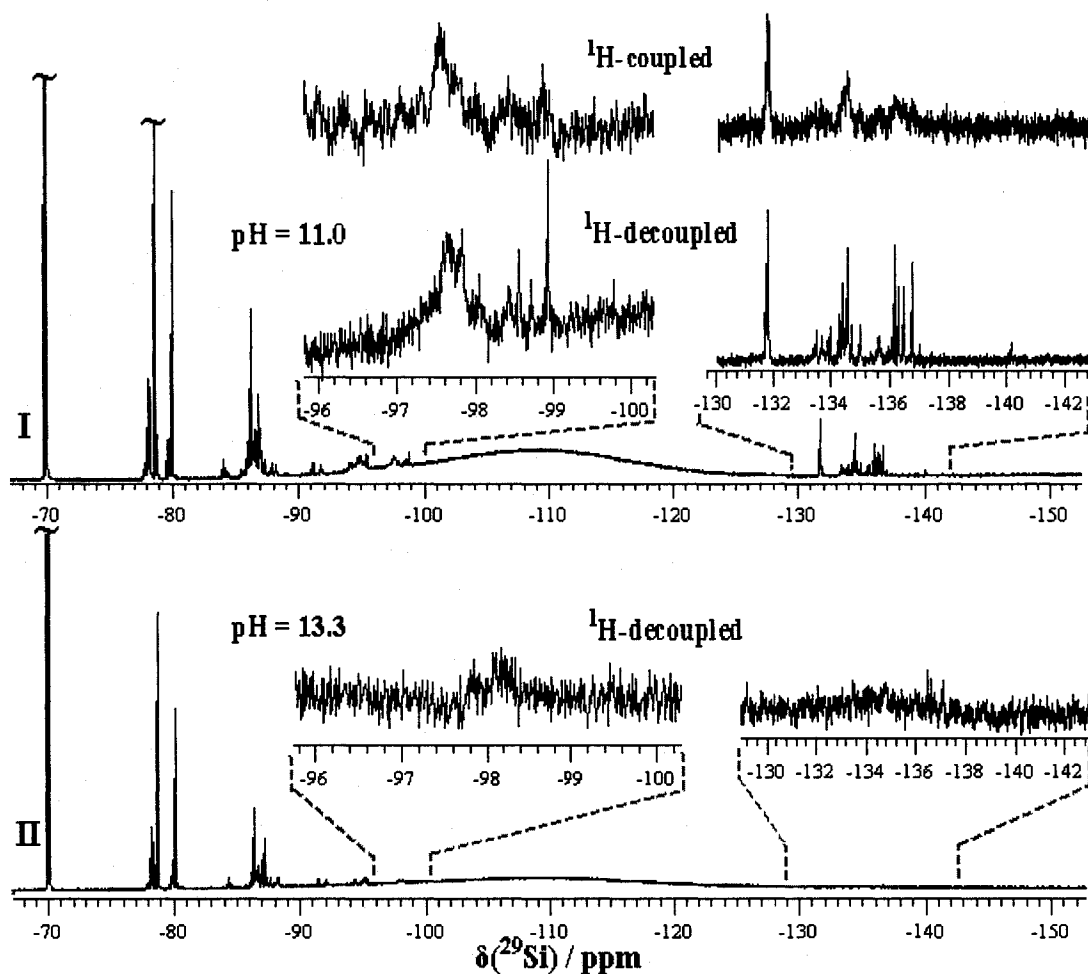


Figure 3.3.2 Silicon-29 NMR (99.28 MHz) spectra of sodium silicate solution containing $0.087 \text{ mol kg}^{-1}$ D-apiose, 0.17 mol kg^{-1} SiO_2 (70.0 atom% ^{29}Si) and (I) 0.21 mol kg^{-1} NaOH or (II) 0.46 mol kg^{-1} NaOH. Expansions of the hypercoordinated spectral regions are also shown in the corresponding insets. PH uncertainty is ± 0.3 units. All spectra were recorded at 278 K using $1100 \pi/2$ pulses and a 60 s inter pulse delay.

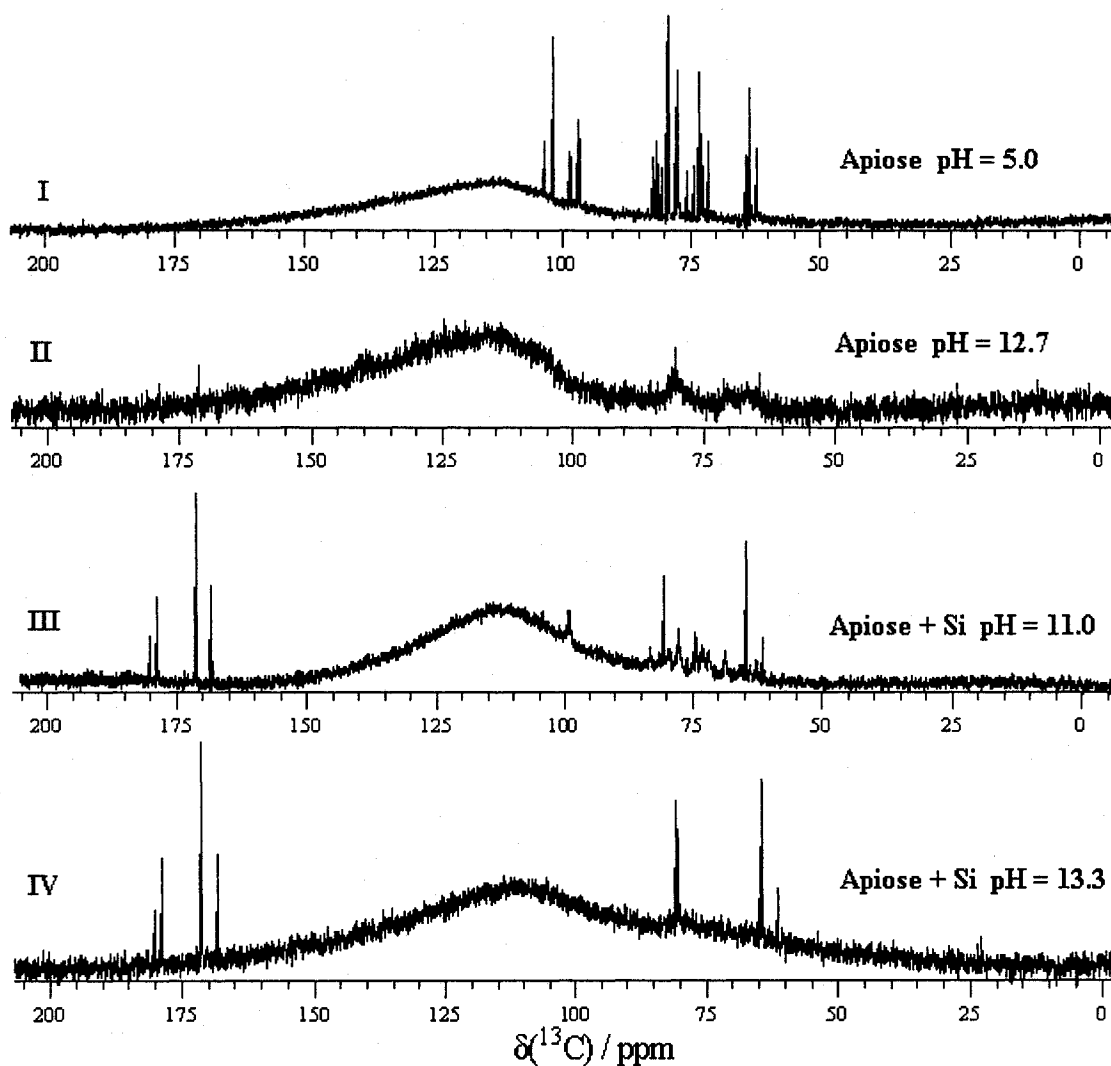


Figure 3.3.3 Carbon-13 NMR (125.66 MHz) spectra of aqueous solutions containing: (I) $0.087 \text{ mol kg}^{-1}$ D-apiose; (II) $0.087 \text{ mol kg}^{-1}$ D-apiose and 0.16 mol kg^{-1} NaOH; (III) $0.087 \text{ mol kg}^{-1}$ D-apiose, 0.17 mol kg^{-1} SiO_2 and 0.21 mol kg^{-1} NaOH and (IV) $0.087 \text{ mol kg}^{-1}$ D-apiose, 0.17 mol kg^{-1} SiO_2 and 0.46 mol kg^{-1} NaOH. PH uncertainty is ± 0.3 units. Spectra were recorded at 278 K using $8000 \pi/2$ pulses and a 10 s inter-pulse delay. Artificial line broadening is 5.0 Hz. The broad peak at *ca.* 110 ppm in each spectrum is attributable to the Teflon FEP NMR tube liner.

evidenced by the broad ^{13}C resonances in spectrum (II). Additionally, new peaks appear in the 165-180 ppm region. Spectra (III) and (IV) correspond to the silicate-containing solutions represented in Figures 3.3.2(I) and (II), respectively. From comparison of spectra (II) and (III), it is apparent that the addition of sodium silicate causes narrowing of several apiofuranose resonances in the 60-85 ppm and 95-105 ppm regions, which would suggest that the formation of apiofuranose-Si complexes may hinder rapid interchange between the apiofuranose isomers and, indeed, favour the existence of certain isomers over others. Four sharp ^{13}C NMR resonances are now clearly resolved in the 165-180 ppm region and apparently associated with three equally sharp signals at *ca.* 62, 65 and 80 ppm. Spectrum (IV) shows that these seven signals dominate the ^{13}C spectrum as pH is increased, and that all peaks associated with apiofuranose have since disappeared. It is noteworthy that the disappearance of the apiofuranose ^{13}C peaks in spectrum (IV) coincides with the disappearance of hypercoordinated ^{29}Si NMR peaks in spectrum II of Figure 3.3.2. Therefore, apiofuranose binds with aqueous silicon to give hypercoordinated Si complexes, but the high pH alteration products of apiofuranose clearly do not.

We have confirmed that the *cis*-2,3-dihydroxy apiofuranose residues of the

plant cell wall polysaccharide RG-II are capable of binding Si in aqueous solution. We cannot identify the high pH alteration products of free apiose at this time, but it is important to note that the apiofuranosyl residue of RG-II would be less susceptible to decomposition since it is bound through glycosyl linkages to other sugars and thus unable to undergo facile ring-opening. Moreover, as part of this study, we determined that the *trans*-dihydroxy analogue of *cis*-2,3-dihydroxy apiofuranose, 2,5-anhydro-D-mannitol, is *incapable* of binding aqueous Si and thus obtained further confirmation that furanoidic molecules must possess *cis*-dihydroxy functionality in order to complex silicon [87]

3.4 Isolation and Purification of Red Wine RG-II

We attempted isolation of rhamnogalacturonan-II from red wine over a two-year period using the procedures discussed in Chapter 2, and ultimately produced 1.2 g of a silver white solid with mushroom-like texture.

Figure 3.4.1 shows a typical uronic acid assay of boric acid-containing RG-II concentrate that has been eluted from a Sephadex size exclusion chromatography (SEC) column. The corresponding ^{11}B NMR spectra are shown in Figure 3.4.2. Uronic acid fractions containing RG-II would be expected to yield a ^{11}B NMR peak at *ca.* -10 ppm

[109b]. Fraction A from the SEC column exhibited no such signal and is thought to consist of a mixture of large pigment molecules. The combined fractions B and C did yield a ^{11}B -diester signal at -9.70 ppm, suggesting that they correspond to the dimeric RG-II borate diester complex and monomeric RG-II, respectively.

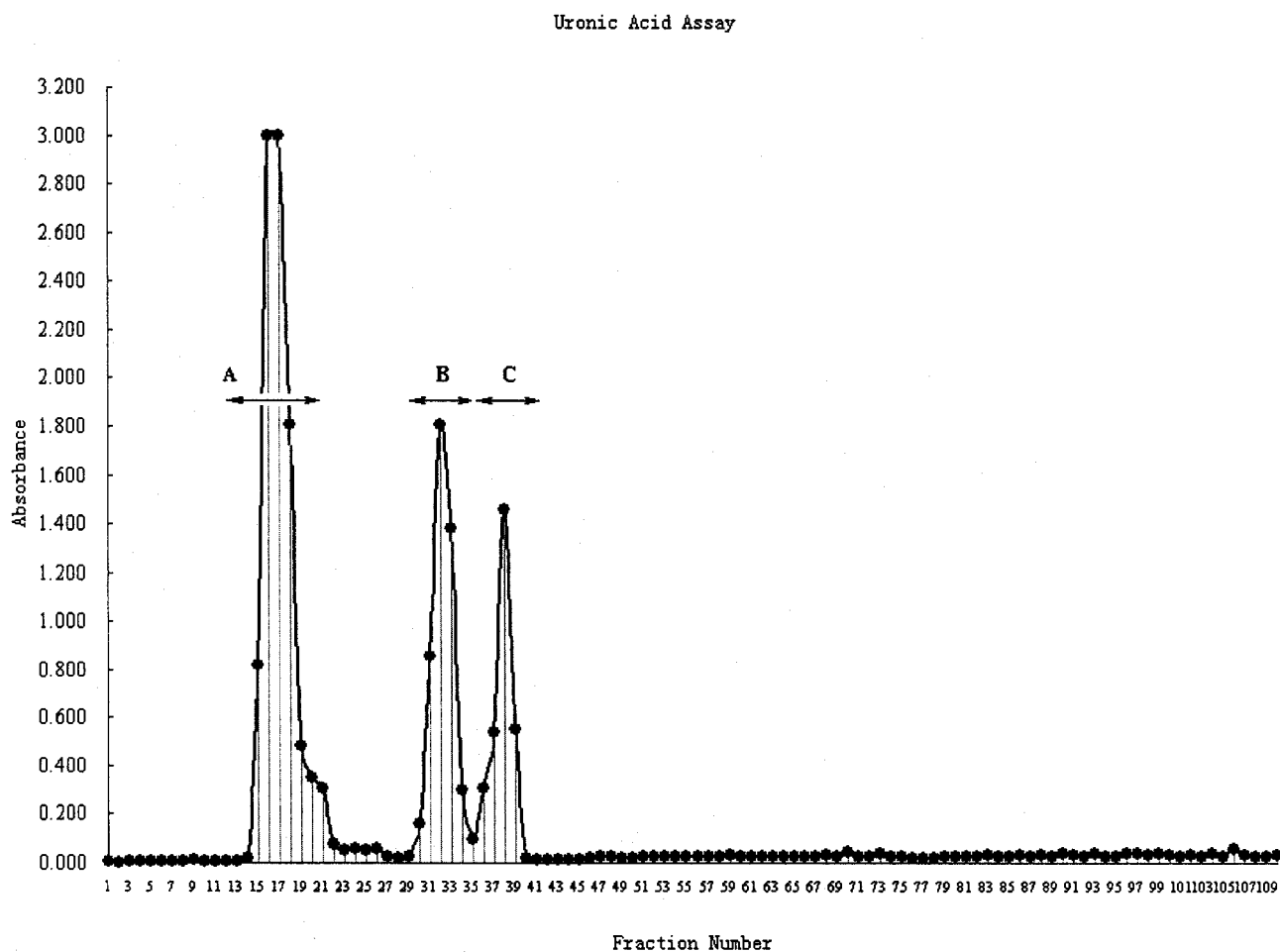


Fig. 3.4.1 Uronic acid assay chromatogram of boric acid-containing RG-II concentrate eluted at pH 5.2 from the Sephadex G-75 SEC column. Molecules elute from the column in order of descending weight. The fraction represented by peak A was pink in colour and did not yield a ^{11}B NMR signal corresponding to borate-diester. (Refer to figure 3.4.2(II).) It was therefore attributed to macromolecular wine pigments. Fractions B and C are respectively assigned to dimeric RG-II borate diester complex and monomeric RG-II.

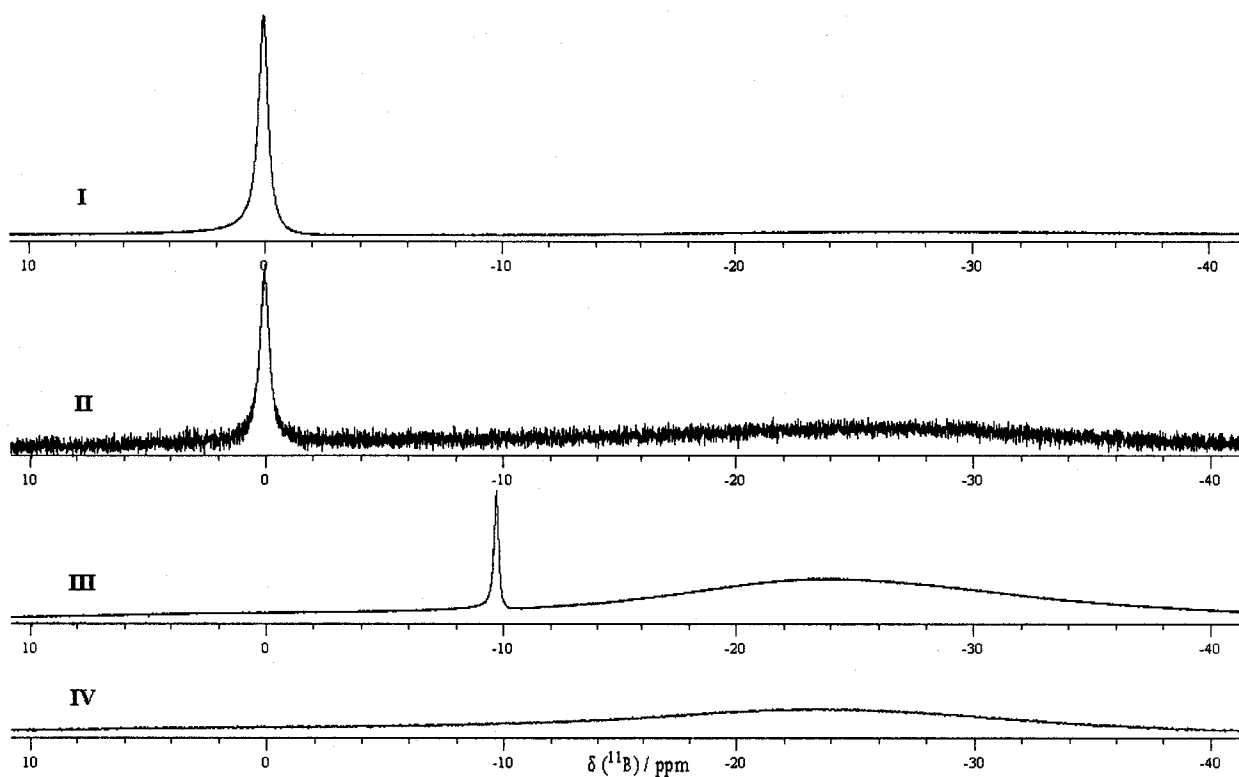


Fig 3.4.2 Boron-11 NMR (160.33MHz) spectra of: (I) 0.20 M boric acid; (II) SEC fraction A (eluant no. 14-22); (III) SEC fractions B plus C (eluant no. 29-40); and (IV) SEC fractions B plus C after acidification/dialysis to remove boric acid. Spectra were recorded at 296 K using 6000-10000 $\pi/2$ pulses, 2 s inter-pulse delay and gated H-decoupling. The NMR peak at 0 ppm corresponds to boric acid, whereas the signal at -9.9 ppm is assigned to borate diester complex. The broad resonance centered at *ca.* -23 ppm arises from the glass borosilicate NMR tube.

The absence of ^{11}B NMR signals in Figure 3.4.2(IV) confirms that all the boron was eliminated from fractions B and C following acid hydrolysis of the dimeric RG-II borate diester and subsequent dialysis of the mixture. The resulting boron-free product

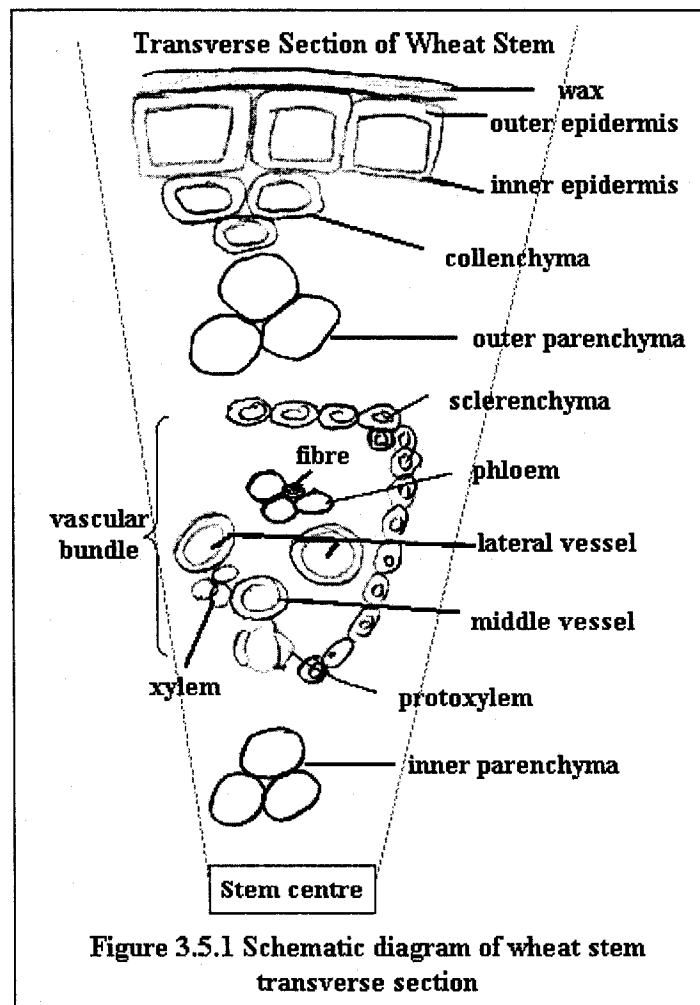
was then lyophilized from D₂O. Once sufficient “RG-II product” had been collected it was added to a solution of sodium silicate, which was then analyzed by ²⁹Si NMR spectroscopy. At 295K, on the ²⁹Si NMR spectrum of the 0.314 ml solution containing 0.125 M SiO₂ (98.7 atom% ²⁹Si), 0.128 M NaOH and 180.1 mg “RG-II”, no organosilicate signal representing the evidence of Si-RG-II complexation was detected. Electrospray-ionization and matrix-assisted laser desorption/ionization mass spectroscopy of the “RG-II product” revealed only a small proportion of high molecular weight polysaccharides, and the maximum weight was only half the 4713 KDa molar mass reported for monomeric RG-II [117b]. It would appear, therefore, that the RG-II decomposed at some point during the extraction and purification process – as did its apiofuranose residues.

3.5 Effect of silicon on cell wall morphology of wheat (*Triticum aestivum*)

Here, we report the results of a series of experiments designed to determine silicon’s influence on the cell wall structure of wheat plants (*Triticum aestivum*).

As represented in Figure 3.5.1, a mature wheat plant stem has a single outer layer of epidermal cells that is covered in waxes and other secretions; next inwards are

layers of collenchyma cells plus “inner” and “outer” layers of parenchyma cells located on either side of the vascular bundles. The vascular bundles have an outer casing of thick-walled sclerenchyma cells which surround the phloem tubes and their companion cells, xylem vessels, and, at the core, large metaxylem vessels with ribbed walls. The centre of the stem is either hollow or composed of parenchyma cells.



In a preliminary study, summarized in Appendix I, the outer parenchyma cells were found to be more responsive than other cell types to the Si level of the nutrient medium. In addition, the wall thickness of other cell types could not be measured as accurately: a) The waxy coating of epidermal cells made it difficult to discern the wall boundaries. b) Collenchyma cells did not occur in all stem segments, and wall thickness varied within individual cells. c) Phloem and xylem vessels were too thin for light microscope measurements. d) The ribbing of metaxylem cell walls led to large measurement uncertainties. Figure 3.5.2 shows representative SEM photographs of outer parenchyma cells in paraffin-embedded stem sections. It is plainly evident that parenchyma cell walls in the plant grown without silicon (-Si) are *significantly* thicker than those in plant grown with silicon (+Si).

Quantitative measurements of the outer parenchyma cell walls are summarized in Table 3.5.1. Regardless of the method used for tissue embedding, -Si cell walls were consistently 4 to 5 times thicker than +Si cell walls in parenchyma from the set of plants grown in February 2004. Briefly soaking the -Si stem sections in 0.020 mM silicic acid did not significantly have an effect on their cell wall thickness.

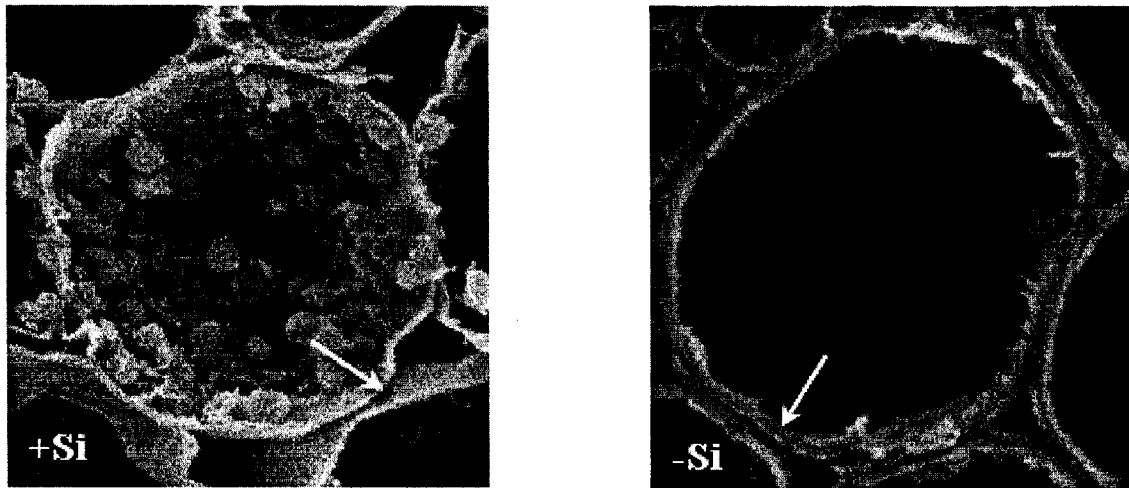


Figure 3.5.2. SEM photographs of representative parenchymal cells in paraffin embedded stem sections prepared from +Si and –Si samples of the February set of mature wheat plants. Each photograph is 50 μm along an edge.

In order to test the reproducibility of the above results, a second set of plants was grown in June 2004. Stem sections were embedded in paraffin and the thickness of the parenchyma cell walls measured using SEM. The findings are summarized in Table 3.5.1 and indicate that, for this trial, there was *no difference* in cell wall thickness between the +Si and –Si plants. Curiously, the wall thicknesses were intermediate between those measured for the +Si and –Si plants in the February set of plants. Representative samples from the June plants were digested and analyzed by ICP to determine whether they might have been contaminated with adventitious Si in the nutrient medium. The results are shown in Table 3.5.2.

Table 3.5.1. Wall thickness of outer parenchyma cells in mature wheat stems.

Plants ^a		Mean cell wall thickness ^b /μm	Ratio -Si / +Si	Ratio (-Si to +Si) / +Si
February set ^c (embedded in plastic resin)	-Si	1.58 ± 0.19	4.2 ± 2.1	-
	+Si	0.38 ± 0.19		
	(-Si to +Si)	1.54 ± 0.12	N/A	4.1 ± 2.1
February set ^c (embedded in paraffin)	-Si	1.48 ± 0.25	5.3 ± 1.4	-
	+Si	0.28 ± 0.06		
June set ^d (embedded in paraffin)	-Si	0.79 ± 0.12	0.93 ± 0.25	-
	+Si	0.85 ± 0.19		

^a Plants were grown in medium containing 0.020 mM silicic acid (+Si), in Si-free medium (-Si), or in Si-free medium and soaked for 30 min in 0.020 mM silicic acid and 0.50 mM CaSO₄ at pH 6.0 (-Si to +Si). ^b Average of 5-20 measurements, listed fully in Appendix II. ^c Measured using light microscopy. ^d Measured using SEM.

Table 3.5.2. ICP-AES analysis of the June set of wheat samples ($\mu\text{g/g}$ oven-dry weight). Data are given for duplicate samples. ^{a, b}

	Stem		Leaves		Flower	
+Si						
<i>Al</i>	< 5.0	< 5.0	< 5.0	< 5.0	< 5.0	< 5.0
<i>B</i>	2.19	2.12	18.62	17.81	7.05	7.10
<i>Ca</i>	2830.31	2939.83	15699.9	15333.6	2386.04	2343.65
<i>Cu</i>	2.97	2.99	8.38	9.43	2.87	2.95
	46.91	48.75	140.28	138.50	44.16	46.53
<i>K</i>	33389.7	33045.5	29476.6	28320.1	11023.2	10704.1
<i>Mg</i>	927.28	973.30	2605.90	2620.55	1410.88	1411.86
<i>Na</i>	85.24	88.19	118.89	115.69	24.17	22.87
<i>Si</i>	238.60	215.28	595.53	590.90	39.91	39.03
-Si						
<i>Al</i>	5.03	< 5.0		5.81	< 5.0	< 5.0
<i>B</i>	2.30	2.07		15.16	6.11	6.25
<i>Ca</i>	2205.76	1796.60		8306.48	1003.10	998.27
<i>Cu</i>	3.17	3.03		7.36	2.71	2.58
	49.88	47.41		120.27	45.60	45.63
<i>K</i>	43137.9	40660.4		35665.5	15355.6	15171.8
<i>Mg</i>	994.62	878.63		2536.00	1248.86	1227.28
<i>Na</i>	117.93	105.99		120.65	49.05	47.02
<i>Si</i>	30.30	25.58		36.32	10.28	11.66
-Si to +Si						
<i>Al</i>	< 5.0	< 5.0	< 5.0	< 5.0	12.96	< 5.0
<i>B</i>	2.59	2.25	17.08	< 2.0	6.37	6.14
<i>Ca</i>	3601.25	3151.31	12546.7	12235.4	1911.12	1902.84
<i>Cu</i>	3.82	3.21	8.74	8.73	4.08	3.78
<i>Fe</i>	40.14	34.34	116.17	109.91	46.09	42.23
<i>K</i>	50987.1	48301.8	31782.4	31160.6	17520.8	18009.1
<i>Mg</i>	1027.10	906.39	2409.34	2467.81	1256.16	1254.19
<i>Na</i>	156.14	125.90	99.16	93.09	47.44	46.91
<i>Si</i>	168.37	143.35	351.37	352.19	269.54	286.28

^a Plants grown in medium containing 0.020 mM silicic acid (+Si), in Si-free medium (-Si), or in Si-free medium and soaked for 60 min in 0.020 mM silicic acid and 0.50 mM CaSO_4 (-Si to +Si). ^b Uncertainties are ($\mu\text{g/g}$): Al, 5.0; B, 0.1; Ca, 0.1; Cu, 0.02; Fe, 0.1; K, 5.0; Mg, 0.1; Na, 0.1; and Si, 0.5.

The data in Table 3.5.2 reveal that the silicon content of the –Si wheat is far from zero. The *relative* silicon content in the –Si plants, expressed as a fraction of that in the +Si plants, is 12% for the stems, 6% for the leaves and 28% for the seed crown. It would appear that the June plants were indeed contaminated by some extraneous Si source which might possibly account for the discrepancy between the two data sets. (Elemental assay was not performed on the February set of wheat plant.)

Interestingly, the relative silicon content of the “(–Si to +Si)” plants – those that were only fed Si 1 h prior to harvesting – rises to 69% for stems, 59% for leaves and an amazing 704% for the crowns. This would imply the existence of an extremely rapid Si transport process in agreement with Casey *et. al.* [50].

Although more work is necessary to verify the above findings, they nonetheless support the hypothesis that Si enhances the well-being of higher plants by improving cell wall integrity (*i.e.*, decreasing wall thickness and permeability) via cross-linking interactions with pectic polysaccharides and/or structural glycoproteins in the primary cell wall.

3.6 Analysis of silicon uptake and excretion in humans

The kinetics of Si uptake and excretion in humans following the oral ingestion of orthosilicic acid was recently characterized by Powell and coworkers [65, 66]. The serum Si concentration was shown to peak at *ca.* 1 h after ingestion, with most of the silicon being excreted in urine within 6 h [65, 66]. The identity of the major Si-containing molecules in the biofluids was not determined, however.

In the present study, a 20 year old male subject drank 500 mL water that contained $2.87 \text{ mmol kg}^{-1} \text{ SiO}_2$ (41.5 mg; 98.7 atom% ^{29}Si) and $3.03 \text{ mmol kg}^{-1} \text{ NaOH}$ at pH 7.9. Figure 3.6.1(I) shows that mono- and disilicic acid were the sole Si-containing species detected in the ingested water, within the detection limit of $1.1 \text{ mg L}^{-1} \text{ Si}$. (As a comparison, Figure 3.6.1(II) shows the ^{29}Si NMR spectrum of a $3.47 \text{ mmol kg}^{-1}$ silicic acid solution at pH 5.2. The ratio of monomeric to dimeric silicic acid in each solution is 11.5:1 and 10:1, respectively.)

The Si concentrations of the blood serum and urine samples that were collected from the test subject are listed in Tables 3.6.1 and 3.6.2.

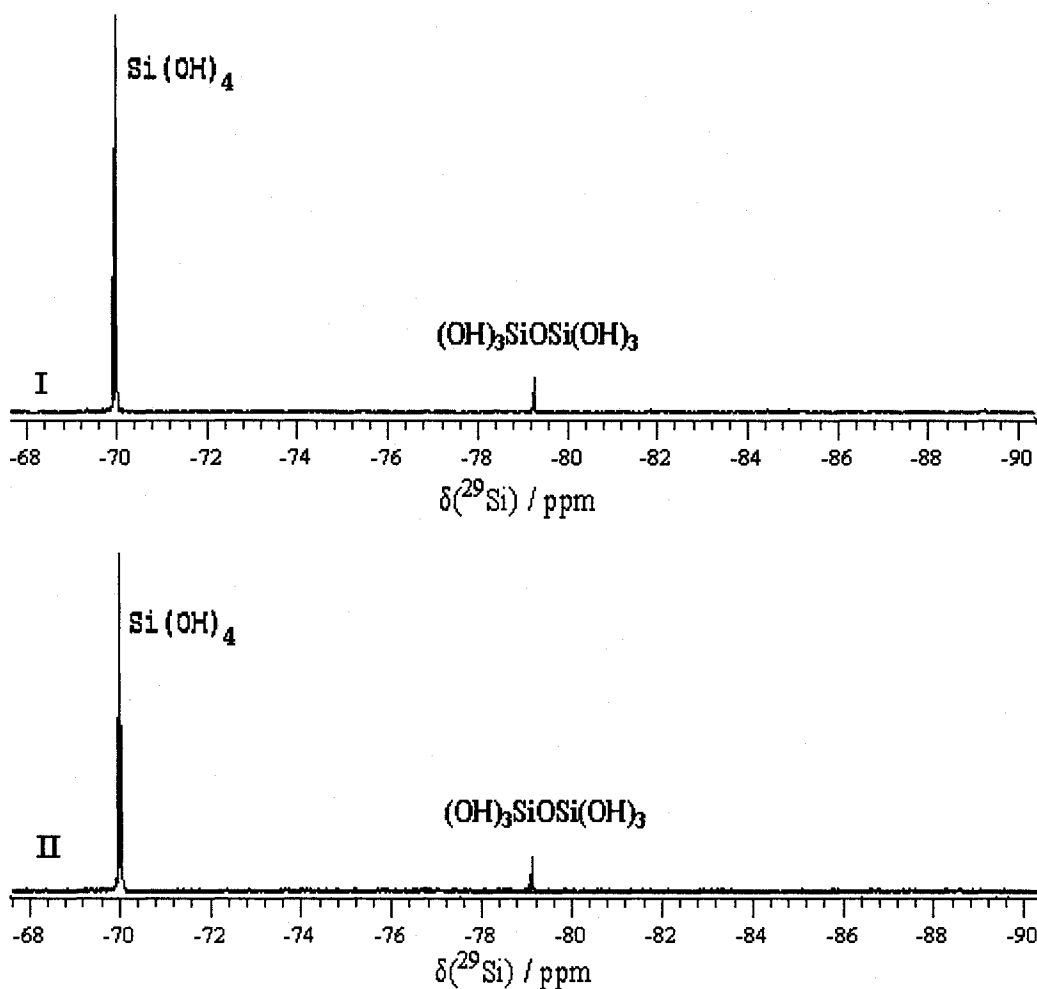


Figure 3.6.1. (I) Silicon-29 NMR (99.31 MHz) spectrum of water ingested by the test subject, containing $2.87 \text{ mmol kg}^{-1} \text{ SiO}_2$ (98.7 atom% ^{29}Si), $3.03 \text{ mmol kg}^{-1} \text{ NaOH}$ and $\text{pH} = 7.9 \pm 0.3$. (II) Silicon-29 NMR (149.00 MHz) spectrum of water that had been autoclaved with amorphous silica (98.7 atom% ^{29}Si) at 150°C for 72 h. The resulting solution contained $3.47 \text{ mmol kg}^{-1} \text{ SiO}_2$ at $\text{pH} = 5.2 \pm 0.3$. The spectra were recorded at 298 K using 800-1000 $\pi/2$ pulses, gated ^1H -decoupling and 100 s inter-pulse delay. Artificial line broadening = 1.0 Hz. Spectral integration reveals that the ratios of monomeric to dimeric silicic acid are (I) 11.5:1 and (II) 10:1.

Table 3.6.1. Silicon concentration of blood serum samples by ICP-OES.

Time post-ingestion / h	Si concentration ^a / $\mu\text{g L}^{-1}$	Weight% of total Si intake ^b
0	93.15	-
0.5	652.96	6.74
1 ^c	1328.65	14.88
1.5	1217.36	13.54
2	1207.47	13.42
3	991.43	10.82
4	574.49	5.80
5	516.45	5.10
6	437.97	4.15

^a Accuracy (determined by spiking and recovery experiments) is $101.4 \pm 3.7\%$ for Si in serum. Precision in measurements is $107.8 \pm 7.9\%$ for Si in serum. ^b Values are calculated assuming 5.0 L blood in subject. ^c This serum sample was examined by ²⁹Si NMR.

Table 3.6.2. Silicon concentration of urine samples by ICP-OES.

Urine collection	Si concentration ^a / mg L ⁻¹	Weight% of total Si intake ^b
24 h before ²⁹ Si ingestion	7.11	-
0 h before ²⁹ Si ingestion	7.55	-
0-3 h after ²⁹ Si ingestion ^b	70.49	36.09
3-6 h after ²⁹ Si ingestion ^c	20.04	12.59

^a Accuracy (determined by spiking and recovery experiments) is $102.0 \pm 5.7\%$ for Si in urine. Precision in measurements is $102.7 \pm 4.1\%$ for Si in urine. ^b The weight of this collection was 238.04 g. Silicon-29 NMR was conducted on this sample. ^c The weight of this collection was 418.30 g.

As shown in Figure 3.6.2(I), the serum Si concentration peaked at one hour following sample ingestion and, thereafter, slowly returned towards the baseline concentration. Figure 3.6.3(I) indicates that the silicon was readily eliminated in the urine. During the first 3 h following sample ingestion, 36.1% of the Si was excreted. Another 12.6% was eliminated over the next three hours. Thus, 48.7% of the total ingested silicon was eliminated from the body within six hours. Moreover, about 47% of the ingested silicon had been absorbed from the digestive tract within three hours of

ingestion (Table 3.6.1), indicating that Si in the form of orthosilicic acid is readily absorbed and readily excreted. These results are entirely consistent with data reported by Powell *et al.* [65, 66].

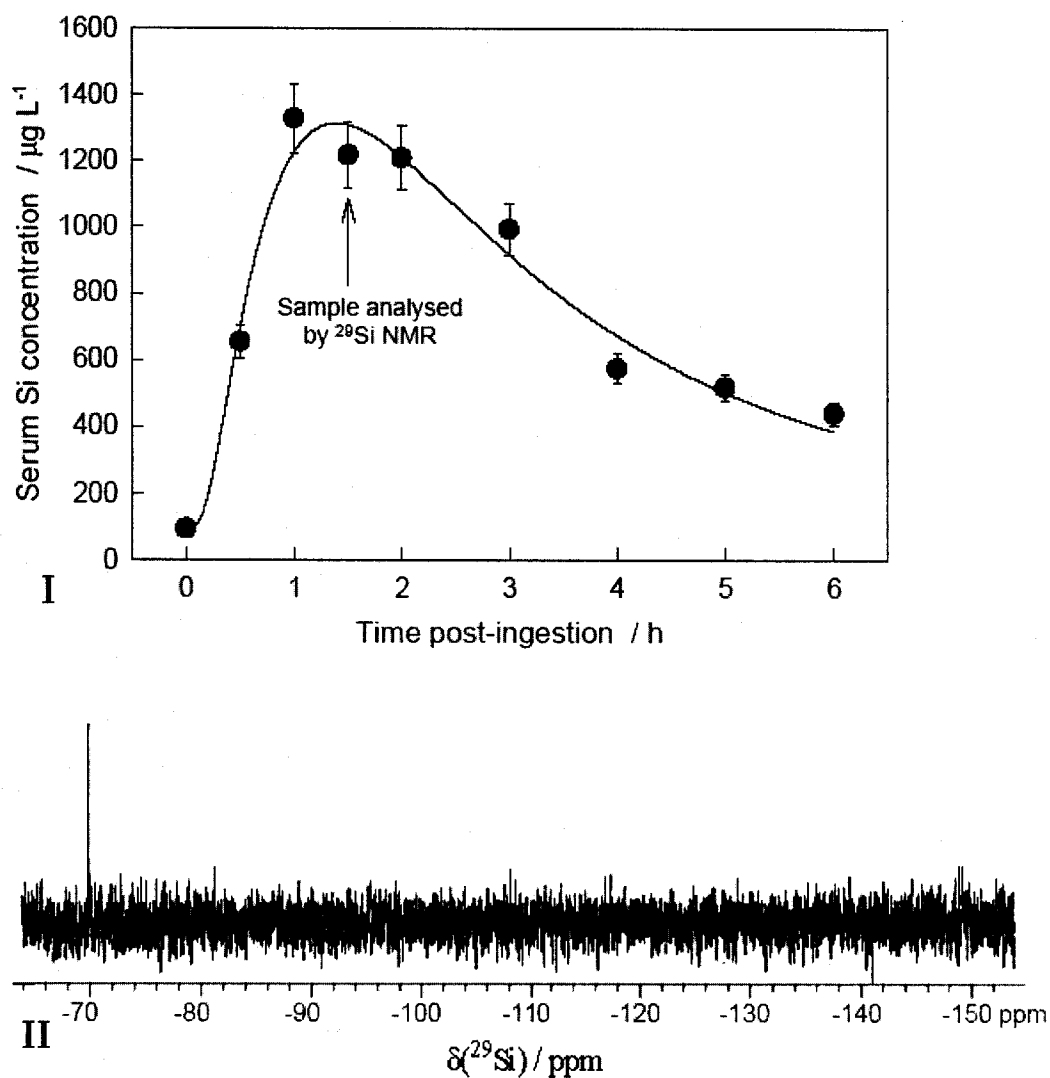


Figure 3.6.2 (I) Serum silicon concentration following ingestion of 41.5 mg Si (98.7 atom% ^{29}Si) in 500 mL type-I water. (II) Silicon-29 NMR (149.00 MHz) spectrum of serum collected 1.5 h after Si ingestion, acquired at 298 K using 2024 $\pi/2$ pulses, gated ^1H -decoupling and a 81 s inter-pulse delay.

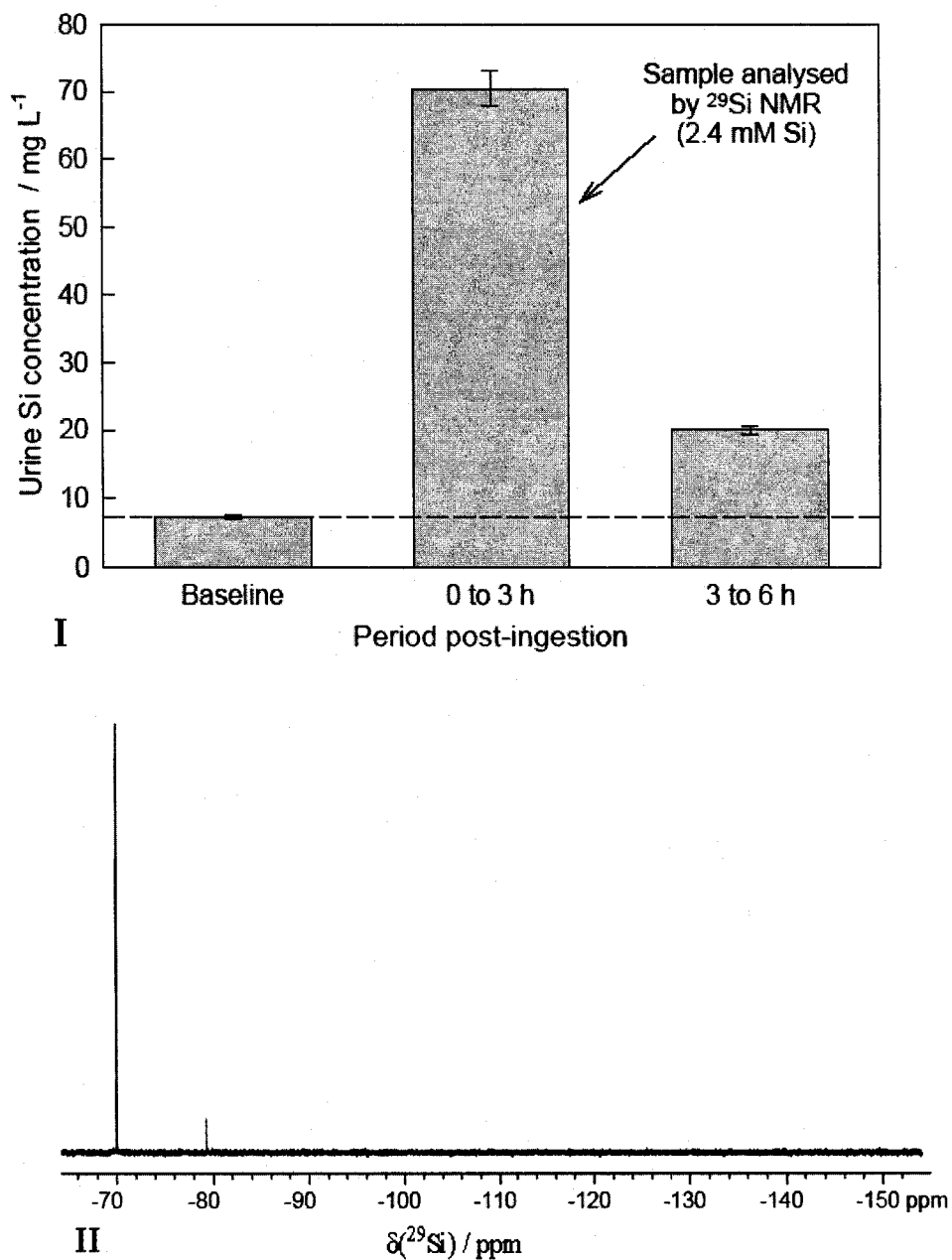


Figure 3.6.3 (I) Urine silicon concentration following ingestion of 41.5 mg Si (98.7 atom% ²⁹Si) in 500 mL type-I water. (II) Silicon-29 NMR (149.00 MHz) spectrum of urine collected during the 3 h period following Si ingestion, acquired at 298 K using 878 $\pi/2$ pulses, gated ¹H-decoupling and a 81 s inter pulse delay.

The serum and urine samples which were most concentrated in silicon were analyzed using ^{29}Si NMR. Figure 3.6.2(II) shows that, within the spectral detection limit of *ca.* $270 \mu\text{g L}^{-1}$ Si, only monosilicic acid was present in the serum 1.5 h after Si ingestion. Figure 3.6.3(II) shows that the exclusive Si-containing species excreted in urine over the 3 h following Si ingestion were mono- and disilicic acid. In this case, the detection limit is *ca.* $536 \mu\text{g L}^{-1}$ Si. Importantly, no signals corresponding to organosilicate species were detected in either spectrum.

These results represent the first reliable speciation of Si-containing molecules in human biofluids, and demonstrate that mono- and disilicic acid are the predominant species that are actively absorbed and excreted. No other Si-containing molecules were detected. We note that similar findings were obtained for the Si-rich xylem exudate of wheat plants [50]. Indeed, if organosilicate species exist at all in organisms, the likely place to find them will be in polyol-rich environments with comparatively low water activity, such as plant cell walls and the extracellular matrix of connective tissues in mammals.

Conclusions

The mechanism proposed by Zhou *et al.* [35] to explain silicatein's interaction with silicon is not supported by the present findings. No interaction was observed between aqueous silicon and the histidine and serine residues of trypsin – even at elevated pH and in the presence of 4-aminobutanol.

We report the first-ever evidence of an amino acid, 2,3-*trans*-3,4-*cis*-3,4-dihydroxy-L-proline (DHP), spontaneously forming stable hypercoordinated Si complexes in aqueous solution. Silicon is complexed by the free amino acid, as well as by DHP in an oligopeptide, under alkaline through to neutral pH conditions. The resulting organosilicates are *anti,anti*, *anti,syn* and *syn,syn* diastereomers of the monomeric *bis*(diolato)hydroxo silicon complex $[(\text{DHP})_2\text{SiOH}]^-$. Standard amino acid assays have been shown to mistake DHP for *trans*-3-hydroxyproline and, thus, it is possible that dihydroxyproline is not actually as rare as we think. The present findings indicate that a logical place to look for DHP would be hydroxyproline-rich macromolecules such as collagen and plant cell wall glycoproteins (*e.g.*, silaffins) that are suspected of interacting with silicon.

Apiofuranose also reacts with aqueous Si at high pH conditions, yielding monomeric *bis*(diolato)hydroxo silicon species with *anti,anti*, *anti,syn* and *syn,syn* ligand configuration. This observation bolsters our hypothesis that many of the benefits conferred by silicon on plants are due to an increase in cell wall integrity that arises when silicon (acting much like boron) cross-links pectic RG-II molecules via their apiofuranose residues. Although we were unable to test this theory *in-vitro* using extracted RG-II from red wine, *in-vivo* studies conducted with hydroponically grown wheat (*Triticum aestivum*) indicate that silicon deficiency indeed causes significant (up to 400%!) swelling of parenchyma cell walls.

The dominant Si-containing species in human blood and urine are mono- and disilicic acid. No evidence was found of organosilicate complexes. Silicic acid is readily absorbed and excreted in humans. Serum Si concentration reaches a maximum level about one hour after silicic acid is orally ingested, and most of the silicon is excreted within 6 h.

Future Work

A number of follow-up studies are suggested by our findings:

- Characterize the alteration products resulting from the long term interaction of 2,3-*trans*-3,4-*cis*-3,4-dihydroxy-L-proline (DHP) with aqueous silicon at elevated pH, and explore if aqueous Si might play a role in proline hydroxylation/dehydroxylation reactions.
- Seek evidence for the existence of DHP in hydroxyproline-rich macromolecules such as collagen and plant cell wall glycoproteins that are suspected of interacting with silicon.
- Obtain 200+ mg of pure, well-characterized RG-II with which to investigate its interaction with aqueous silicon.
- Conduct a comprehensive study of silicon's influence on plant cell wall structure compared with that of boron, taking every precaution to eliminate extraneous sources of both elements.

References

1. Liebau, F. (1985) *Structural Chemistry of Silicates*. Springer-Verlag, Berlin.
2. Evered, D. and Connor, M.O. (1986) Introduction to silicon chemistry and biochemistry. In *Silicon Biochemistry*, CIBA Foundation Symposium 121, Evered, D. and O'Connor, M. eds. Wiley, New York.
3. (a) Birchall, J.D., Exley, C. and Chappell, J.S. (1989) Acute toxicity of aluminum to fish eliminated in silicon-rich acid waters. *Nature* 338:146-148. (b) Birchall, J.D. (1995) The essentiality of silicon in biology. *Chem. Soc. Rev.* 24:351-357.
4. (a) Epstein, E. (1999) Silicon. *Annu. Rev. Plant Physiol. Plant Mol. Biol.* 50:641-664. (b) Epstein, E. (1994) The anomaly of silicon in plant biology. *Proc. Natl. Acad. Sci. USA* 91:11-17.
5. Carlisle, E.M. (1986) *Silicon as an essential trace element in animal nutrition*. In *Silicon Biochemistry*, CIBA Foundation Symposium 121, Evered, D. and O'Connor, M. eds. Wiley, New York, 123-139.
6. Peluso, M.R. and Schneeman, B.O. (1994) A food-grade silicon dioxide is hypocholesterolemic in the diet of cholesterol-fed rats. *J. Nutr.* 124:853-860.
7. Burton, A.C., Cornhill, J. F. and Canham, P. B. (1980) Protection from cancer by 'silica' in the water supply of U.S. cities. *J. Environ. Pathol. Toxicol.* 4:31-40.
8. Belles, M., Sanchez, D.J., Gomez, M., Corbellam, J. and Domingo, J.L. (1998) Silicon reduces aluminum accumulation in rats: relevance to the aluminum hypothesis of Alzheimer disease. *Alzheimer Dis. Assoc. Disord.* 12:83-7.
9. Carlisle, E. M. (1981) Silicon in bone formation. In *Silicon and Siliceous Structures*

- in Biological Systems* Simpson, T.L. and Volcani, B.E. eds. Springer-Verlag, New York, 69-94.
10. (a) Perry, C.C. and Keeling-Tucker, T. (2000) Model studies of the precipitation of silica in the presence of aluminium; implications for biology and industry. *J. Inorg. Biochem.* 78:331–339 (b) (1998) Aspects of the bioinorganic chemistry of silicon in conjunction with the biometals calcium, iron and aluminium. *J. Inorg Biochem.* 69:181-91.
 11. (a) Jugdaohsingh, R., Reffitt, D.M., Oldham, C., Day, J.P., Fifield, L.K., Thompson, R.P. and Powell, J.J. (2000) Oligomeric but not monomeric silica prevents aluminum absorption in humans. *Am. J. Clin. Nutr.* 71:944-949. (b) Exley, C. (1998) Silicon in life: A bioinorganic solution to bioorganic essentiality. *J. Inorg Biochem.* 69:139-144.
 12. Knight, C.T.G. and Kinrade, S.D. (2001) A primer on the aqueous chemistry of silicon. *Stud. Plant Sci. (Silicon in Agriculture)*. Datnoff, L.E., Snyder, G.H. and Korndörfer, G.H. eds. Elsevier, New York) 8:57-84.
 13. Sjöberg, S., Nordin, A. and Ingri, N. (1981) Equilibrium and structural studies of silicon (IV) and aluminum (III) in aqueous solution. *Mar. Chem.* 10:521–532.
 14. Iler, R.K. (1979) *The Chemistry of Silica*, Wiley, New York, 40–46.
 15. Knight, C.T.G. (1988) A two-dimensional silicon-29 NMR spectroscopic study of the structure of the silicate anions present in an aqueous potassium silicate solution. *J. Chem. Soc., Dalton Trans.* 1457-1460.
 16. Kinrade, S.D. and Swaddle, T.W. (1988) Silicon-29 NMR studies of aqueous silicate

- solution. 1. Chemical shifts and equilibria. *Inorg. Chem.* 27:4253-4259.
17. Perry, C.C. and Keeling-Tucker, T. (2000) Biosilicification: the role of the organic matrix in structure control. *J. Biol. Inorg. Chem.* 5:537-550
 18. Muller-Werner, E.G. (ed) (2003) Silicon Biomineralization. *Progress in Molecular and Subcellular Biology*, Vol. 33, Springer-Heidelberg.
 19. Lowenstam, H.A. (1981) Biominerals. *Science*, 211:1126-1131
 20. Perry, C.C. (2003) Silicification: The processes by which organisms capture and mineralize silica. *Rev. Mineral. Geochem.* 54: 291-327
 21. Falciatore, A. and Bowler, C. (2002) Revealing the molecular secrets of marine diatoms. *Annu. Rev. Plant. Biol.* 53:109-130.
 22. Simpson, T.L. and Volcani, B.E. eds. (1981) In *Silicon and Siliceous Structures in Biological Systems*. Springer, New York, 15-42.
 23. Round, F.E., Crawford, R.M. and Mann, D.G. (1990) In *The Diatoms: Biology & Morphology of the Genera*. Cambridge University Press, New York.
 24. (a) Hecky, R.E., Mopper, K., Kilham, P. and Degens, T. (1973) Amino-acid and sugar composition of diatom cell-walls. *Mar. Biol.* 19:323-331. (b) Swift, D.M. and Wheeler A.P. (1992) Evidence of an organic matrix from diatom biosilica. *J. Phycol.* 28:202-209.
 25. Kröger, N., Deutzmann, R. and Sumper, M. (1999) Polycationic peptides from diatom biosilica that direct silica nanosphere formation. *Science* 286:1129-1132.
 26. Kröger, N., Deutzmann, R., Bergsdorf, C. and Sumper, M. (2000) Species-specific polyamines from diatoms control silica morphology. *Proc. Natl. Acad. Sci.* 97:

14133–14138.

27. Kröger, N., Deutzmann, R. and Sumper, M. (2001) Silica-precipitating Peptides from Diatoms: The chemical structure of silaffin-1a from *cylindrotheca fusiformis*. *J. Biol. Chem.* 276:26066–26070.
28. Patwardhan, S.V. and Clarkson, S.J. (2003) Silicification and biosilicification: Part 5 An investigation of the silica structures formed at weakly acidic pH and neutral pH as facilitated by cationically charged macromolecules. *Mater. Sci. Eng., C* 23:495–499.
29. Vrieling, E.G., Gieskes, W.W.C. and Beelen, T.P.M. (1999) Silicon deposition in diatoms: Control by the pH inside the silicon deposition vesicle. *J. Phycol.* 35:548-559.
30. Kröger, N., Deutzmann, R. and Sumper, M. (2002) Self-assembly of highly phosphorylated silaffins and their function in biosilica morphogenesis. *Science* 298: 584–586.
31. (a) Sumper, M. (2002) A phase separation model for the nanopatterning of diatom biosilica. *Science* 295:2430-2433. (b) Sumper, M. (2004) Biomimetic patterning of silica by long-chain polyamines. *Angew. Chem. Int. Ed.* 43:2251-2254 (c) Brunner, E., Lutz, K. and Sumper, M. (2004) Biomimetic synthesis of silica nanospheres depends on the aggregation and phase separation of polyamines in aqueous solution. *Phys. Chem. Chem. Phys.* 6: 854–857
32. (a) Mizutani, T., Nagase, H., Fujiwara, N. and Ogoshi, H. (1998) Silicic acid polymerization catalyzed by amines and polyamines. *Bull. Chem. Soc. Jpn.*

- 71:2017-2022. (b) Pohnert, G. (2002) Biomineralization in Diatoms Mediated through Peptide- and Polyamine-Assisted Condensation of Silica. *Angew. Chem. Int. Ed.* 41:3167-3169
33. Poulsen, N., Sumper, M. and Kröger, N. (2003) Biosilica formation in diatoms: Characterization of native silaffin-2 and its role in silica morphogenesis. *Proc. Natl. Acad. Sci.* 100: 12075–12080.
34. Shimizu, K., Cha, J., Stucky, G.D. and Morse, D.E. (1998) Silicatein α : Cathepsin L-like protein in sponge biosilica. *Proc. Natl. Acad. Sci.* 95: 6234–6238.
35. (a) Zhou, Y., Shimizu, K., Cha, J.N., Stucky, G.D. and Morse, D.E., (1999) Efficient catalysis of polysiloxane synthesis by silicatein α requires specific hydroxy and imidazole functionalities. *Angew. Chem. Int. Ed.* 38: 780 -782. (b) Cha, J. N., Shimizu, K., Zhou, Y., Christiansen, S.C., Chmelka, F.C., Stucky, G.D. and Morse, D.E. (1999) Silicatein filaments and subunits from a marine sponge direct the polymerization of silica and silicones in vitro. *Proc. Natl. Acad. Sci. USA* 96:361-365.
36. Krasko, A., Lorenz, B., Batel, R., Schroder, H.C., Muller, I.M. and Muller, W.E.G. (2000) Expression of silicatein and collagen genes in the marine sponge *Suberites domuncula* is controlled by silicate and myotrophin. *Eur. J. Biochem.* 67:4878-4887.
37. Tacke, R. (1999) Milestones in the Biochemistry of Silicon: From basic research to biotechnological applications. *Angew. Chem. Int. Ed.* 38:3015-3018.
38. Sahai, N. (2004) Calculation of ^{29}Si NMR shifts of silicate complexes with carbohydrates, amino acids, and MuHicarboxylic acids: Potential role in biological

- silica utilization. *Geochim. Cosmochim. Acta*, 68:227–237.
39. Richmond, K.E. and Sussman, M. (2003) Got silicon? The non-essential beneficial plant nutrient. *Curr. Opin. Plant Biol.* 6: 268-273.
 40. Lux, A., Luxova, M., Hattori, T., Inanaga, S. and Sugimoto, Y. (2002) Silicification in sorghum (*Sorghum bicolor*) cultivars with different drought tolerance. *Physiol. Plant* 115:87-92.
 41. Epstein, E. (2000) The discovery of the essential elements. In *Discoveries in Plant Biology* vol. 3, Kung, S.D. and Yang, S.F. eds. World Scientific Publishing, Singapore.
 42. Epstein, E. (2001) Silicon in Plants: Facts vs. Concepts. *Stud. Plant Sci. (Silicon in Agriculture)*. Datnoff, L.E., Korndörfer, G. and Snyder, G. eds. Elsevier, New York) 8:133-147.
 43. Neumann, D. and Nieren, Z.U. (2001): Silicon and heavy metal tolerance of higher plants. *Phytochemistry* 56:685-692.
 44. Simkiss, K. and Wilbur, K.M. (1989) *Biom mineralization: Cell Biology and Mineral Deposition*. Academic Press, San Diego.
 45. Korndörfer, G.H. and Lepsch, I. (2001) Effect of silicon on plant growth and crop yield. *Stud. Plant Sci. (Silicon in Agriculture)*. Datnoff, L., Korndörfer, G. and Snyder, G. eds. Elsevier, New York) 8:133-147.
 46. Ma, J.F., Miyake, Y. and Takahashi, E. (2001) Silicon as a beneficial element for crop plants. *Stud. Plant Sci. (Silicon in Agriculture)*, Datnoff, L., Korndörfer, G. and Snyder, G. eds. Elsevier, New York) 8:17-39.

47. Raven, J.A. (2003) Cycling silicon-the role of accumulation in plants. *New Phytol.* 158:419–421.
48. Sangster, A.G. and Hodson, M.J. (1992) Silica in higher plants. In *Silicon Biochemistry*, CIBA Foundation Symposium 121, Evered, D. and O'Connor M. eds. Wiley, New York.
49. Mayland, H.F., Johnson, D.A., Asay, K.H. and Read, J.J. (1993) Ash, carbon isotope discrimination, and silicon as estimators of transpiration efficiency in crested wheatgrass. *Aust. J. Plant. Physiol.* 20:361-369.
50. Casey, W.H., Kinrade, S.D., Knight, C.T.G., Rains, D.W. and Epstein, E. (2004) Aqueous silicate complexes in wheat, *Triticum aestivum* L. *Plant Cell Environ.* 27: 51–54.
51. Ma, J.F., Tamai, K., Ichii, M. and Wu, G.F. (2002) A rice mutant defective in Si uptake. *Plant Physiol.* 130:2111-2117.
52. Takahashi, E., Ma, J.F. and Miyake, Y. (1990) The possibility of silicon as an essential element for higher plants. *Comments Agric. Food Chem.* 2:99-122.
53. (a) Harrison, C.C. (1996) Evidence for intramineral macromolecules containing protein from plant silicas. *Phytochemistry* 41:37-42. (b) Inanaga, S. and Okasaka, A. (1995) Calcium and silicon binding compounds in cell walls of rice shoots. *Soil. Sci. Plant Nutr.* 41:103-110. (c) Inanaga, S., Okasaka, A. and Tanaka, S. (1995) Does silicon exist in association with organic compounds in rice plants? *Soil. Sci. Plant Nutr.* 41:111-117.
54. Kauss, H., Seehaus, K., Franke, R., Gilbert, S., Dietrich, R.A. and Kröger, N. (2003)

- Silica deposition by a strongly cationic proline-rich protein from systemically resistant cucumber plants. *The Plant Journal* 33, 87–95.
55. (a) Carlisle, E. M. (1972). Silicon: An Essential Element for the Chick. *Sci.* 619-621.
(b) Schwarz, K. and Milne, D.B. (1972). Growth-promoting effects of silicon in rats. *Nature* 239:333-334.
56. Carlisle, E.M. (1974) Silicon as an essential element. *Fed. Proc.* 33:1758-1766.
57. Carlisle, E.M. (1976) In *vivo* requirement for silicon in articular cartilage and connective tissue formation in the chick. *J. Nutr.* 106:478-484.
58. Carlisle, E.M. (1980) A silicon requirement for normal skull formation. *J. Nutr.* 10:352-359.
59. Carlisle, E.M. (1980) Biochemical and morphological changes associated with long bone abnormalities in silicon deficiency. *J. Nutr.* 10:1046-1056.
60. Carlisle, E.M. and Alpenfels, W.F. (1984). The role of silicon in proline synthesis. *Fed. Proc.* 43:680.
61. Carlisle, E.M., Beger, J.M. and Alpenfels, W.F. (1981). A silicon requirement for propyl hydroxylase activity. *Fed. Proc.* 40:866.
62. Carlisle, E.M. (1982) The nutritional essentiality of silicon. *Nutr. Rev.* 40:193-198.
63. Calomme, M.R. and Vanden Berghe D.A. (1997) Supplementation of calves with stabilized orthosilicic acid. Effect on the Si, Ca, Mg, and P concentrations in serum and the collagen concentration in skin and cartilage. *Biol. Trace Elem. Res.* 56:153-65.
64. Cefali, E.A., Nolan, J.C., McConnell, W.R. and Walters, D.L. (1996) Bioavailability

- of silicon and aluminum from Zeolite A in dogs. *Int. J. Pharm.* 127:147-154.
65. Reffitt, D.M., Jugdaohsingh, R., Thompson, R.P.H. and Powell, J.J. (1999) Silicic acid: its gastrointestinal uptake and urinary excretion in man and effects on aluminium excretion. *J. Inorg. Biochem.* 76:141–6.
66. Jugdaohsingh, R., Anderson, S.H., Tucker, K.L., Elliott, H., Kiel, D.P., Thompson, R.P. and Powell, J.J. (2002) Dietary silicon intake and absorption. *Am. J. Clin. Nutr.* 75:887–93.
67. Schiano, A., Eisinger, F., Detolle, P., Laponche, A.M., Brisou, B. and Eisinger, J. (1979) Silicon, bone tissue and immunity. *Rev. Rhum. Mal. Osteoartic.* 46:483–486.
68. Eisinger, J. and Clairet, D. (1993) Effects of silicon, fluoride, etidronate and magnesium on bone mineral density: a retrospective study. *Magnes. Res.* 6:247–249.
69. Hott, M., DePollak, C., Modrowski, D. and Marie, P.J. (1993) Short-term effects of organic silicon on trabecular bone in mature ovariectomized rats. *Calcif. Tissue Int.* 53:174–9.
70. Rico, H., Gallego-Largo, J.L. and Hernandez, E.R. (2000) Effects of silicon supplementation on osteopenia induced by ovariectomy in rats. *Calcif. Tissue Int.* 66:53–5.
71. Jugdaohsingh, R., Tucker, K.L., Qiao, N., Cupples, L.A., Kiel, D.P. and Powell, J.J. (2004) Dietary silicon intake is positively associated with bone mineral density in men and premenopausal women of the Framingham Offspring cohort. *J. Bone Miner. Res.* 19:297-307.
72. Reffitt, D.M., Ogston, N., Jugdaohsingh, R., Cheung, H.F., Evans, B.A., Thompson,

- R.P., Powell, J.J. and Hampson, G.N. (2003). Orthosilicic acid stimulates collagen type 1 synthesis and osteoblastic differentiation in human osteoblast-like cells in vitro. *Bone* 32:127-135.
73. TanBeeWan, A., Duivenvoorden, W.C.M. and Kinrade, S.D. (2004) Effect of silicon on survival and cell proliferation in human osteoblast-like Saos-2 cells. *Bone* 34: S13-S14.
74. (a) Lewin, J. and Reimann, B.E.F. (1969) Silicon and plant growth. *Ann. Rev. Plant Physiol.* 20:289–308. (b) Iler, R.K. (1979) *The Chemistry of Silica*, Wiley, New York, 866.
75. Herreros, B., Carr, S.W. and Klinowski, J. (1994) 5-Coordinate Si compounds as intermediates in the synthesis of silicates in nonaqueous media. *Science* 263: 1585-1587.
76. Laine, R.M. (1996) Processable aluminosilicate alkoxide precursors from metal oxides and hydroxides. The oxide one-pot synthesis process. *J. Mater. Chem.* 6: 1441-1443.
77. Blohowiak, K.Y. (1994) SiO₂ as a starting material for the synthesis of pentacoordinate silicon complexes.1. *Chem. Mater.* 6: 2177-2192.
78. Hoppe, M.L., Laine, R.M., Kampf, J., Gordon, M.S. and Burggraf L.W. (1993) Ba[Si(OCH₂CH₂O)₃], A hexaalkoxysilicate synthesized from SiO₂. *Angew. Chem. Int. Ed. Engl.* 32: 287-289.
79. Sedeh, I.F. and Sjöberg, S. (a) (1992) Equilibrium and structural studies of silicon (IV) and aluminum (III) in aqueous-solution.30. Aqueous complexation between

- silicic-acid and some ortho-diphenolic and triphenolic compounds. *Acta Chem. Scand.* 46:933-940. (b) (1993) Equilibrium and structural studies of silicon (IV) and aluminum (III) in aqueous-solution .31. Aqueous complexation between silicic-acid and the catecholamines dopamine and L-DOPA. *J. Inorg. Biochem.* 50: 119-132.
80. Weiss, A. and Harvey, D.R. (1964) Water-stable cationic complexes of silicic acid with 1-hydroxypyridine n-oxide. *Angew. Chem. Int. Edit.* 3:698.
81. (a) Sjöberg, S., Ingri, N., Nenner, A.M. and Öhman, L.O. (1985) Equilibrium and structural studies of silicon (IV) and aluminum (III) in aqueous-solution .12. A potentiometric and Si-29-NMR study of silicon tropolonates *J. Inorg. Biochem.* 24, 267-277. (b) Evans, D.F., Parr, J. and Wong, C.Y. (1992) Nuclear magnetic resonance studies of silicon (IV) complexes in aqueous-solution. 2. Tris-tropolonato and tris-3-hydroxypyridin-4-onato complexes. *Polyhedron* 11, 567-572.
82. Kinrade, S.D., Del Nin, J.W., Schach, A.S., Sloan, T.A., Wilson, K.L. and Knight, C.T.G. (1999) Stable five- and six-coordinated silicate anions in aqueous solution. *Science* 285:1542-1545.
83. Kinrade, S.D., Hamilton, R.J., Schach, A.S. and Knight, C.T.G. (2001) Aqueous hypervalent silicon complexes with aliphatic sugar acids. *J. Chem. Soc., Dalton Trans.* 961-963.
84. Kinrade, S.D., Schach, A.S., Hamilton, R.J. and Knight C.T.G. (2001) NMR evidence of pentaoxo organosilicon complexes in dilute neutral aqueous silicate solutions. *J. Chem. Soc., Chem. Commun.* 1564-1565.

85. Kubicki, J.D. and Heaney, J.D. (2003) Molecular orbital modeling of aqueous organosilicon complexes: Implications for silica biomineralization. *Geochim. Cosmochim. Acta* 67:4113–4121.
86. Benner, K., Klufers, P. and Vogt, M. (2003) Hydrogen-bonded sugar alcohol trimers as hexadentate silicon chelators in aqueous solution. *Angew. Chem. Int. Ed.* 42:1058–1062.
87. Kinrade, S.D., Deguns, E.W., Gillson, A.M. E. and Knight C.T.G. (2003) Complexes of pentaoxo and hexaoxo silicon with furanoidic vicinal cis-diols in aqueous solution. *J. Chem. Soc., Dalton Trans.* 3713–3716.
88. Kinrade, S.D., Balec, R. J., Schach, A.S.S, Wang, J. and Knight, C.T.G. (2004) The structure of aqueous pentaoxo silicon complexes with *cis*-1,2-dihydroxycyclopentane and furanoidic vicinal cis-diols. *J. Chem. Soc., Dalton Trans.* 3241-3243.
89. Kinrade, S.D., Gillson, A.M.E. and Knight, C.T.G. (2002) Silicon-29 NMR evidence of a transient hexavalent silicon complex in the diatom *Navicula pelliculosa*. *J. Chem. Soc., Dalton Trans.* 307-309.
90. (a) Lambert, J.B., Lu, G., Singer, S.R. and Kolb, V.M. (2004) Silicate Complexes of Sugars in Aqueous Solution. *J. Am. Chem. Soc.* 126:9611-9625. (b) Munoz, A. and Lamande, L. (1992) Borate esters of alditols - synthesis, structure and stability in aqueous-solution. *Carbohydrate Res.* 225:113-121.
91. (a) Dunitz, J.D., Hawley, D.M., Miklos, D., White, D.N.J., Berlin, Y., Marusic, R. and Prelog, V. (1971) Metabolic products of microorganisms .95. Structure of boromycin. *Helv. Chim. Acta* 54:1709. (b) Nakamura, H., Iitaka, Y., Kitahara, T.,

- Okazaki, T., Okami, Y. (1977) Structure of aplasmomycin. *J. Antibiot. (Tokyo)* 30: 714-719. (c) Irschik, H., Schummer, D., Gerth, K., Hofle, G., Reichenbach, H. (1995) The tartrolons, new boron-containing antibiotics from a myxobacterium, *Sorangium cellulosum*. *J. Antibiot. (Tokyo)* 48: 26-30
92. Chen, X., Schauder, S., Potier, N., Dorsselaer, A.V., Pelczer, I., Bassler, B.L. and Hughson, F.M. (2002) Structural identification of a bacterial quorum-sensing signal containing boron. *Nature* 415: 545-549.
93. O'Neill, M.A., Ishii, T., Albersheim, P. and Darvill, A.G. (2004) Rhamnogalacturonan II: structure and function of a borate cross-linked cell wall pectic polysaccharide. *Annu. Rev. Plant Biol.* 55:109–139.
94. (a) Coradin, T. and Livage, J. (2001) Effect of some amino acids and peptides on silicic acid polymerization. *Colloids Surf. B Biointerfaces* 21:329–336. (b) Belton, D., Paine, G., Patwardhan, S.V. and Perry, C.C. (2004) Towards an understanding of (bio)silicification: the role of amino acids and lysine oligomers in silicification. *J. Mater. Chem.* 14:2231–2241.
95. Hamilton, R. and Kinrade, S.D., unpublished work.
96. London, R.E. and Gabel, S.A. (2002) Formation of a Trypsin-Borate-4-Aminobutanol ternary complex. *Biochemistry* 41:5963-5967.
97. Transue, T.R., Krahn, J.M., Gabel, S.A., DeRose, E.F. and London, R.E. (2004) X-ray and NMR Characterization of Covalent Complexes of Trypsin, Borate, and Alcohols. *Biochemistry* 43:2829-2839.
98. Mauger, A.B. (1996) Naturally Occurring Proline Analogues. *J. Nat. Prod.*

- 59:1205-1211.
99. (a) Karle, I.L., Daly, J.W. and Witkop, B. (1969)
2,3-*cis*-3,4-*trans*-3,4-dihydroxy-l-proline - mass spectrometry and x-ray analysis.
Science 164:1401-1402. (b) Nakajima, T. and Volcani, B.E. (1969)
3,4-Dihydroxyproline - a new amino acid in diatom cell walls. *Science* 164:
1400-1401.
100. Buku, A., Faulstich, H., Wieland T. and Dabrowski, J. (1980)
2,3-*trans*-3,4-*trans*-3,4-dihydroxy-l-proline - an amino-acid in toxic peptides of
amanita-virosa mushrooms - (mushroom toxins-virotaxins-dihydroxyproline). *Proc.*
Natl. Acad. Sci. USA 77:2370-2371.
101. Taylor, S.W., Waite, J.H., Ross, M.M., Shabanowitz, J. and Hunt, D.F. (1994)
trans-2,3-*cis*-3,4-Dihydroxyproline, a new naturally occurring amino acid, is the
sixth residue in the tandemly repeated consensus decapeptides of an adhesive protein
from *Mytilus edulis*. *J. Am. Chem. Soc.* 116:10803-10804.
102. Strausberg, R.L. and Link, R.P. (1990) Protein-based medical adhesives. *Tibtech*
8:53-57.
103. Waite, J.H. and Tanzer, M.L. (1981) Polyphenolic substance of *Mytilus-edulis* - novel
adhesive containing l-DOPA and hydroxyproline. *Science* 212:1038-1040.
104. Waite, J.H., Housley, T.J. and Tanzer, M.L. (1985) Peptide repeats in a mussel glue
protein - theme and variations. *Biochemistry* 24: 5010-5014.
105. Taylor, C.M. and Weir, C.A. (2000) Synthesis of the repeating decapeptide unit of
Mefp1 in orthogonally protected form. *J. Org. Chem.* 65:1414-1421.

- 106.(a) Ridley, B., O'Neill, M.A. and Mohnen, D. (2001). Pectin: structure, biosynthesis, and oligogalacturonide-related signaling. *Phytochemistry* 57:929–67. (b) Willats, W.G., McCartney, L., Mackie, W. and Knox, J.P. (2001) Pectin: cell biology and prospects for functional analysis. *Plant Mol. Biol.* 47:9–27.
- 107.Perez, S., Rodriguez-Carvajal, M.A., Doco, T. (2003) A complex plant cell wall polysaccharide: rhamnogalacturonan II. A structure in quest of a function. *Biochimie* 85:109–121.
- 108.Darvill, A.G, McNeil, M. and Albersheim, P., (1978) Structure of plant cell walls. VIII. A new pectic polysaccharide. *Plant Physiol.* 62:418–422.
- 109.(a) Ishii, T., Matsunaga, T., Pellerin, P., O'Neil, M.A., Darvill, A. and Albersheim, P. (1999) The plant cell wall polysaccharide rhamnogalacturonan II self-assembles into a covalently cross-linked dimer. *J. Biol. Chem.* 274:13098–13104. (b) O'Neil, M.A., Warrenfeltz, D., Kates, K., Pellerin, P., Doco, T., Darvill, A.G and Albersheim, P. (1996) Rhamnogalacturonan II, a pectic polysaccharide in the walls of growing plant cell, forms a dimer that is covalently cross-linked by a borate ester. *J. Biol. Chem.* 271:22923-22930.
- 110.Kobayashi, M., Match, T. and Azuma, J. (1996) Two chains of rhamnogalacturonan II are cross-linked by borate-diol ester bonds in higher plant cell walls. *Plant Physiol.* 110:1017-1020.
- 111.Fleischer, A., O'Neill, M.A. and Ehwald, R. (1999) The pore size of nongraminaceous plant cell walls is rapidly decreased by borate ester cross-linking of the pectic polysaccharide rhamnogalacturonan II. *Plant Physiol.* 121:829–838.

112. Match, T. (1997) Boron in plant cell walls. *Plant Soil* 193:59–70.
113. Brown, P.H., Hu, H. (1997) Does boron play only a structural role in the growing tissues of higher plants? *Plant Soil* 196: 211–215.
114. Ishii, T., Matsunaga, T. and Hayashi, N. (2001) Formation of rhamnogalacturonan II-borate dimer in pectin determines cell wall thickness of pumpkin tissue. *Plant Physiol.* 126:1698–1705.
115. Boudart, G., Dechamp-Guillaume, G., Lafitte, C., Ricart, G., Barthe, J.P., Mazau, D. and Esquerre-Tugaye, M.T. (1995) Elicitors and suppressors of hydroxyproline-rich glycoprotein accumulation are solubilized from plant cell walls by endopolygalacturonase. *Eur. J. Biochem.* 232:449–457.
116. Bonilla, I., Mergold-Villasenor, C., Campos, M.E., Sánchez, N., Pérez, H., López, L., Castrejón, L., Sánchez, F. and Cassab, G.I. (1997) The aberrant cell walls of boron-deficient bean root nodules have no covalently bound hydroxyproline/proline-rich proteins. *Plant Physiol.* 115:1329–1340.
117. (a) Doco, T. and Brillouet, J.M. (1993) Isolation and characterization of a rhamnogalacturonan II from red wine. *Carbohydr. Res.* 243:333–343. (b) Pellerin, P., Doco, T., Vidal, S. and Williams, P. (1996) Structural characterization of red wine rhamnogalacturonan II. *Carbohydr. Res.* 290:183–197.
118. Doco, T., Williams, P., Vidal, S. and Pellerin, P. (1997) Rhamnogalacturonan II, a dominant polysaccharide in juices produced by enzymic liquefaction of fruits and vegetables. *Carbohydr. Res.* 297:181–186.
119. Vidal, S., Williams P., Doco, T., Moutouneta, M. and Pellerin P. (2003) The

- polysaccharides of red wine: total fractionation and characterization. *Carbohydrate Polymers* 54 : 439–447.
- 120.Loomis, W.D. and Durst, R.W. (1992) Chemistry and biology of boron. *BioFactors* 3:229–39.
- 121.Kobayashi, M., Ohno, K. and Match, T. (1997). Boron nutrition of cultured tobacco BY-2 cells. II. Characterization of the boron-polysaccharide complex. *Plant Cell Physiol.* 38:676–683.
- 122.Ishii, T., Matsunaga, T., Iwai, H., Satoh, S. and Taoshita, J. (2002). Germanium does not substitute for boron in cross-linking of rhamnogalacturonan II in pumpkin cell wall. *Plant Physiol.* 130:1967–73
- 123.Reffitt, D.M., Jugdaohsingh, R., Thompson, R.P.H. and Powell, J.J. (1999) Silicic acid: its gastrointestinal uptake and urinary excretion in man and effects on aluminium excretion. *J. Inorg. Biochem.* 76:141–147.
- 124.Bellia, J.P., Birchall, J.D. and Roberts, N.B. (1994) Beer: a dietary source of silicon. *Lancet* 343:235.
- 125.Sripanyakorn, S., Jugdaohsingh, R., Elliott, H., Walker, C., Mehta, P., Shoukru, S., Thompson, R.P. and Powell, J.J. (2004) The silicon content of beer and its bioavailability in healthy volunteers. *Br. J. Nutr.* 91:403-9.
- 126.Van Dyck, K., Van Cauwenbergh, R., Robberecht, H. and Deelstra, H. (1999) Bioavailability of silicon from food and food supplements. *Fresenius J. Anal. Chem.* 363:541–4.
- 127.Carlisle, E.M. (1997) Silicon. In *Handbook of Nutritionally Essential Mineral*

- Elements*, O'Dell, B. L., Sunde, R. A. and Dekker, M. eds. New York, 603–618.
128. Pennington, J.A. (1991) Silicon in foods and diets. *Food Addit. Contam.* 8:97–118.
129. Kinrade, S.D. and Swaddle, T.W. (1986) Mechanisms of longitudinal ^{29}Si nuclear magnetic relaxation in aqueous alkali-metal silicate solutions. *J. Am. Chem. Soc.* 108:7159–7162.
130. Glasoe, P.K. and Long, F.A. (1960) Use of glass electrodes to measure acidities in deuterium oxide. *J. Phys. Chem.* 64:188-190.
131. Blumenkr, N. and Asboehan, G. (1973) New method for quantitative-determination of uronic acids. *Anal. Biochem.* 54:484-489.
132. Rafi, M.M. and Epstein, E. (1999) Silicon absorption by wheat (*Triticum aestivum* L.). *Plant Soil* 211:223–230.
133. Johansen, D.A. (1940) *Plant microtechnique*, McGraw-Hill, New York.
134. (a) Kalra, Y.P. and Maynard, D.G. (1991) *Methods Manual for Forest Soil and Plant Analysis*, Forestry Canada Information Report Nor-X-329. (b) Kennan, J.J., Breen, L.L.M., Lane, T.H. and Taylor, R.B. (1999) Methods for detecting silicones in biological matrixes. *Anal. Chem.* 71:3054-3060.
135. Research Ethics Board of Lakehead University
<http://www.lakeheadu.ca/~researchwww/policies/ethics.html>
136. Kinrade, S.D., Maa, K.J., Schach, A.S., Sloan, T.A. and Knight, C.T.G. (1999) Silicon-29 NMR evidence of alkoxy substituted aqueous silicate anions. *J. Chem. Soc., Dalton Trans.* 3149-3151.
137. Knight, C.T.G. and Kinrade, S.D. (2002) Comment on “Identification of precursor

species in the formation of MFI zeolite in the TPAOH-TEOS-H₂O system” *J. Phys. Chem. B* 106: 3329-3332.

138.(a) Karplus, M.J. (1959) Contact electron-spin coupling of nuclear magnetic moments. *J. Chem. Phys.* 30:11-15. (b) Karplus, M.J. (1963) Vicinal proton coupling in nuclear magnetic resonance. *J. Am. Chem. Soc.* 85:2870. (c) Contreras, R.H. and Peralta, J.E. (2000) Angular dependence of spin-spin coupling constants. *Prog. Nucl. Mag. Res. Sp.* 37:321-425.

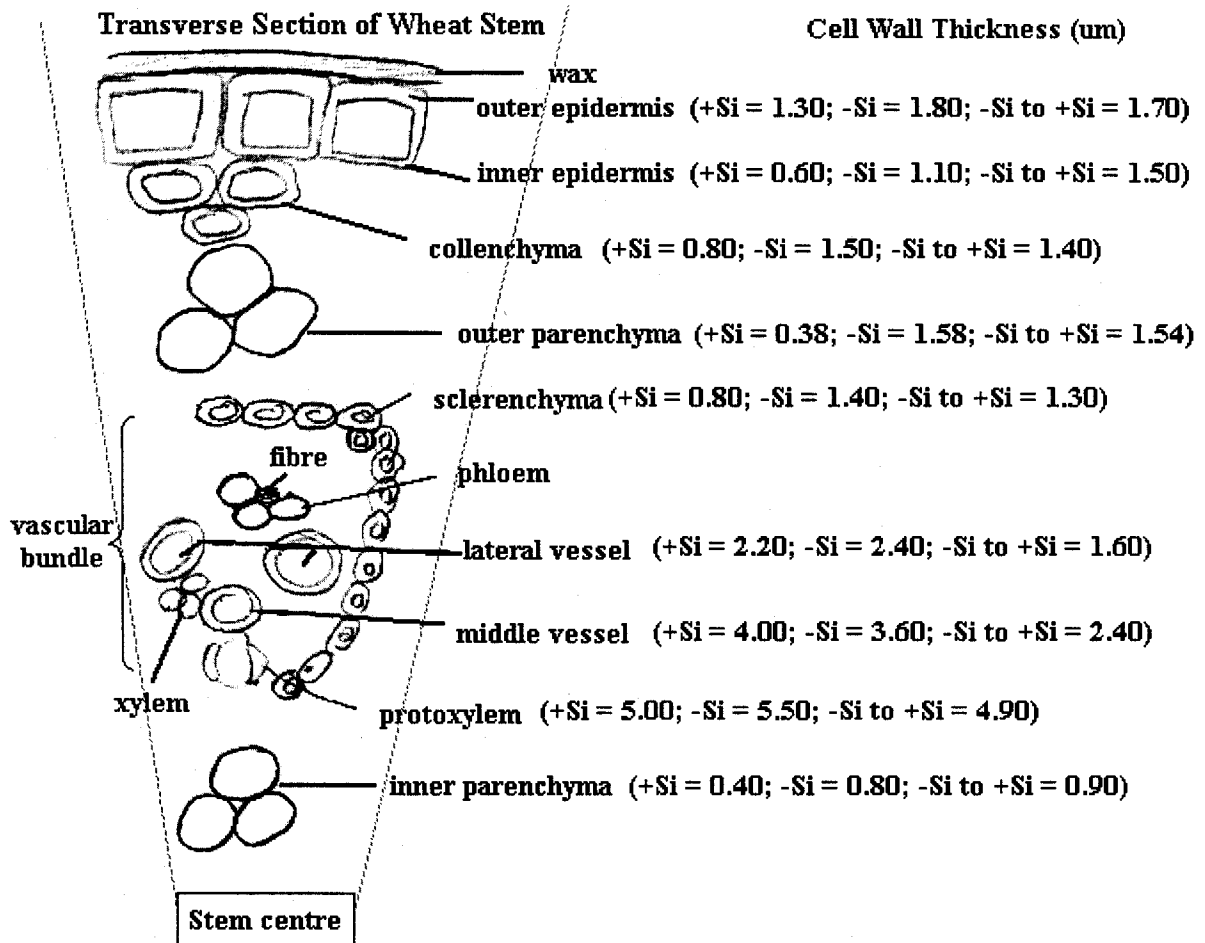
139.(a) Waite, J.H., Housley, T.J. and Tanzer, M.L. (1985) Peptide repeats in a mussel glue protein - theme and variations. *Biochemistry* 24:5010-5014. (b) Hudson, C.B., Robertson, A.V., and Simpson W.R.J., (1968) On the synthesis of 3,4-dihydroxyprolines .I. *cis*-Glycosylation of 3,4-dehydroxyproline derivatives. *Aust. J. Chem.* 21:769.

140.Introduction of biological functionality of collagen:

<http://users.rcn.com/jkimball.ma.ultranet/BiologyPages/C/Collagens.html>,

http://www.rcsb.org/pdb/molecules/pdb4_1.html.

Appendix I. The effect of Si-deficiency on wheat stem cell wall thickness *



* Wheat (*Triticum aestivum*) stem sections were prepared by plastic resin embedded method. Cell wall thickness was measured under light microscope using a x100 oil immersion lens. Uncertainty of each measurement is 0.25 µm. The outer parenchymal cells were noted to be the most responsive with respect to silicon deficiency among all the other measurable cell types.

Appendix II. Parenchyma cell wall thickness measurements – raw data ^a

Plants^b		Cell wall thickness (µm)	Mean value (µm)
Feb. set ^c (embedded in plastic resin)	-Si	1.58, 1.19, 1.58, 1.58, 1.58, 1.58, 1.58, 1.98, 1.58	1.58 ± 0.19
	+Si	0.26, 0.20, 0.26, 0.59, 0.59	0.38 ± 0.19
	-Si to +Si	1.58, 1.19, 1.58, 1.58, 1.58, 1.58, 1.58, 1.58, 1.58, 1.58	1.54 ± 0.12
Feb. set ^c (embedded in paraffin)	-Si	1.19, 1.58, 1.58, 1.58, 1.58, 1.58, 1.58, 1.58, 1.58, 1.58, 1.58, 1.19, 1.19, 1.58, 1.58, 1.19, 0.79, 1.58, 1.58, 1.98	1.48 ± 0.25
	+Si	0.24, 0.24, 0.24, 0.24, 0.24, 0.24, 0.24, 0.24, 0.24, 0.24, 0.32, 0.32, 0.40, 0.40, 0.32, 0.32, 0.24, 0.40, 0.24, 0.40	0.28 ± 0.06
June set ^d (embedded in paraffin)	-Si	0.80, 0.80, 0.90, 0.90, 0.80, 0.50, 0.80, 0.80	0.79 ± 0.12

	+Si	1.00, 0.80, 1.10, 0.80, 0.60, 0.90, 1.00, 0.90, 0.90, 0.40, 1.00, 0.80	0.85 ± 0.19
--	------------	---	-----------------

^a All data were gathered by Dr. David Chapman (Lakehead University.) ^b Plants were grown in medium containing 0.020 mM silicic acid (+Si), in Si-free medium (-Si), or in Si-free medium and soaked for 30 min in 0.020 mM silicic acid and 0.50 mM CaSO₄ at pH 6.0 (-Si to +Si). ^c Measured using light microscope. ^d Measured using SEM.